



Cite this: *Lab Chip*, 2021, **21**, 2658

Recent innovations in cost-effective polymer and paper hybrid microfluidic devices

Wan Zhou, [†]^a Maowei Dou, [†]^a Sanjay S. Timilsina, ^a Feng Xu, ^{*b} and XiuJun Li, ^{*acd}

Hybrid microfluidic systems that are composed of multiple different types of substrates have been recognized as a versatile and superior platform, which can draw benefits from different substrates while avoiding their limitations. This review article introduces the recent innovations of different types of low-cost hybrid microfluidic devices, particularly focusing on cost-effective polymer- and paper-based hybrid microfluidic devices. In this article, the fabrication of these hybrid microfluidic devices is briefly described and summarized. We then highlight various hybrid microfluidic systems, including polydimethylsiloxane (PDMS)-based, thermoplastic-based, paper/polymer hybrid systems, as well as other emerging hybrid systems (such as thread-based). The special benefits of using these hybrid systems have been summarized accordingly. A broad range of biological and biomedical applications using these hybrid microfluidic devices are discussed in detail, including nucleic acid analysis, protein analysis, cellular analysis, 3D cell culture, organ-on-a-chip, and tissue engineering. The perspective trends of hybrid microfluidic systems involving the improvement of fabrication techniques and broader applications are also discussed at the end of the review.

Received 10th May 2021,
Accepted 19th June 2021

DOI: 10.1039/d1lc00414j

rsc.li/loc

^a Department of Chemistry and Biochemistry, University of Texas at El Paso, 500 W University Ave., El Paso, TX 79968, USA. E-mail: xli4@utep.edu

^b Bioinspired Engineering and Biomechanics Center (BEBc), The Key Laboratory of Biomedical Information Engineering of Ministry of Education, School of Life Science and Technology, Xi'an Jiaotong University, Xi'an 710049, PR China

^c Border Biomedical Research Center, Biomedical Engineering, University of Texas at El Paso, 500 West University Ave., El Paso, TX 79968, USA

^d Environmental Science and Engineering, University of Texas at El Paso, 500 West University Ave., El Paso, TX 79968, USA

† These authors contributed equally to this work.

1. Introduction

Microfluidic systems have been developed rapidly in the last two decades, exhibiting numerous applications in chemical, biomedical, biological, and environmental fields.^{1–4} The microfluidic technology was initially applied to manipulate small-volume fluid samples within micro-scale structures, which promoted the development of lab-on-chip (LOC) devices.^{5–7} Microfluidic LOC devices are capable of performing sample preparation, separation, detection, and analysis by integrating multiple components and functional units into a single miniaturized device.^{8,9} In addition,



Wan Zhou

Dr. Wan Zhou received her bachelor's and master's degrees in Chemistry from Zhengzhou University, China, and Ph.D. degree in Chemistry and Biochemistry from the University of Texas at El Paso, USA. She is currently a postdoctoral researcher in the Perelman School of Medicine at the University of Pennsylvania, USA. Her research focuses on developing low-cost microfluidic devices and nanobiosensors for point-of-care disease diagnostics.



Maowei Dou

Dr. Maowei Dou received his Ph. D. degree in Chemistry and Biochemistry from the University of Texas at El Paso, USA. Maowei Dou is currently a research scientist at Thermo Fisher Scientific. His research interests focus on the development of innovative mass spectrometry proteomic reagent products and workflows, and microfluidic bioanalysis techniques.

microfluidic devices can manipulate liquid at microliter or nanoliter levels precisely and efficiently, and allow for high throughput and automation.^{10–12} Associated with a variety of benefits such as small reagent consumption, cost-efficiency, integration, portability, and no need of experienced personnel for operation, such devices have provided a valuable platform in many fields such as human health diagnostics, biomedical applications, controlled drug delivery, and environmental analysis.^{4,13–17} Particularly, the low-cost microfluidic devices have attracted increasing interest in both scientific research and practical applications by providing affordable platforms for point-of-care (POC) applications. The development of low-cost microfluidic platforms is still challenging and demanding, especially in low-resource settings.



Sanjay Sharma Timilsina

Dr. Sanjay Sharma Timilsina from Nepal received his bachelor's and master's degrees in biotechnology from Bangalore University, India and Ph.D. degree in Chemistry and Biochemistry from The University of Texas at El Paso, USA. Currently, he is working as a Postdoctoral fellow in Harvard Medical School and Wyss Institute for Biologically Inspired Engineering at Harvard University. His research interest is focused on low-cost diagnosis of infectious diseases and cancer biomarkers on microfluidic platforms along with development, validation, & quality control of immunoassay and microfluidic medical devices for point-of-care diagnosis.

is focused on low-cost diagnosis of infectious diseases and cancer biomarkers on microfluidic platforms along with development, validation, & quality control of immunoassay and microfluidic medical devices for point-of-care diagnosis.



Feng Xu

Dr. Feng Xu got his Ph.D. degree from Cambridge University and postdoc training at Harvard-MIT HST. He is currently the director of Bioinspired Engineering and Biomechanics Center (BEBC) at Xi'an Jiaotong University, China. His research interest is focused on cell microenvironment engineering and point-of-care testing.

Microfluidic LOC devices can be fabricated from a diverse range of materials, such as silicon, glass, polymeric substrates, cellulosic substrates, and some emerging biomaterials.^{18–22} Based on the number of substrates used in microfabrication, microfluidic LOC devices can be categorized as single-substrate and hybrid (hybrid-substrates) microfluidic devices. Among all hybrid microfluidic devices, polymer and paper hybrid microfluidic devices have been perceived as versatile platforms and applied in many fields, mainly including nucleic acid analysis, protein detection, cellular analysis, 3D cell culture, organ-on-a-chip, and tissue engineering. Although the hybrid microfluidic systems have drawn more and more attention in microfluidic and bioanalytical fields, to the best of our knowledge, there have been no comprehensive reviews on hybrid microfluidic systems. Therefore, this article reviews the recent innovations in the development of hybrid microfluidic devices (e.g., the cost-effective polymer and/or paper-based hybrid microfluidic devices). It mainly focuses on two major types of hybrid devices – polymer/polymer and paper/polymer hybrid microfluidic devices. Readers can refer to different sections directly according to interest.

1.1 Different substrates for the fabrication of microfluidic devices

Microfluidic devices were previously fabricated mostly using silicon and glass, whereas polymer and paper substrates have been subsequently adopted in microfabrication. The applications and limitations of these devices have predominantly relied on the diverse properties of respective materials. Silicon is the first generation of substrates used in microfluidic LOC devices owing to its high thermal conductivity, good chemical resistance, and ease in metal depositing. Silicon-based microfluidic devices have been fabricated leveraging the well-developed semiconductor



XiuJun Li

Dr. XiuJun (James) Li is an Associate Professor in the Department of Chemistry & Biochemistry at the University of Texas at El Paso (UTEP), USA. He received his Ph.D. degree from Simon Fraser University, followed with postdoctoral research at UC Berkeley and Harvard University. His current research interest is centered on the development of innovative microfluidic lab-on-a-chip and nanotechnology for bioanalysis, biomaterial, biomedical engineering, and environmental applications, including but not limited to low-cost diagnosis, hybrid microfluidic devices, nano-sensing, photothermal biosensing, and single-cell analysis.

fabrication strategy.²³ Typically, the microelectromechanical systems (MEMS) technique is adopted to make micro-scale structures with a focus on biochemical analysis.²⁴ However, due to its intrinsic properties (e.g., opacity and hardness) and high manufacturing costs, the broadening demands for microfluidic devices, especially those using optical sensors, could not be satisfied by the silicon-based microfluidic devices.

Afterward, glass was selected to replace silicon in most applications, owing to its optical transparency, chemical inertness, and biocompatibility.²⁵ Moreover, the fabrication strategies of glass microfluidic LOC devices include photolithography, etching, and bonding, which are compatible with MEMS.²⁶ Despite the above advantages, there are several drawbacks associated with glass substrates. Some toxic chemicals are used in the fabrication of glass microfluidic LOC devices, such as piranha solutions to clean glass surfaces prior to bonding, and hydrofluoric acid for glass etching. In addition, glass microfluidic LOC devices require high temperature in the fabrication process. Functionalization of glass chips is necessary to activate the silanol groups *via* chemical reactions, which also increases the complexity and the fabrication cost of glass microfluidic devices.²⁷

As such, cost-effective microfluidic devices made by polymeric materials have quickly become more popular than glass, due to the reduced production costs, flexibility, ease of fabrication, rapid prototyping, and no need for hazardous etching reagents. There are two major types of polymeric substrates used in microfluidic devices: elastomers (e.g., polydimethylsiloxane (PDMS)) and thermoplastics (e.g., poly(methyl methacrylate) (PMMA), polycarbonate (PC), and polystyrene (PS)). PDMS has presently become the most common substrate used in microfabrication, and PDMS-based microfluidic chips are generally fabricated *via* soft lithography. The processing of PDMS chips can be achieved without the aid of cleanroom facilities. The optical transparency also allows PDMS to replace glass at a reduced cost in most optical applications. Moreover, its gas permeability makes PDMS-based microfluidic chips suitable for cellular analysis as well as long-time cell culture. Nonetheless, nonspecific adsorption of biomolecules can compromise the specificity and sensitivity of on-chip assays. Likewise, the degradation of PDMS could occur when exposed to reactive chemicals, and the chemical modification of PDMS surfaces (e.g., plasma treatment) may not be stable during a long period of time.^{28,29}

Different from PDMS, thermoplastics such as PMMA hold good compatibility with the existing mass production infrastructure.³⁰ Numerous prototyping techniques have been developed to make microfluidic devices using thermoplastics, such as laser ablation, injection molding, and micromilling.^{31,32} Thermoplastics microfluidic devices can be fabricated and molded at relatively high temperatures – they are able to withstand high pressure as the materials are rigid below the glass-transition temperature. In addition,

compared to other substrates, thermoplastics exhibit comparable optical properties (e.g., broad visible transmittance and low intrinsic fluorescence), good chemical stability and biocompatibility, and a broader range of mechanical stiffness. Nevertheless, thermoplastics are still not yet the most attractive material used in microfabrication, because of the nonspecific surface adsorption of sample molecules and its impermeability to gas.

Paper-based microfluidic devices have emerged as a low-cost microfluidic platform during the last decade.³³ Many advantages of paper substrates have been found, including extremely low cost, wide availability, disposability, user-friendliness, ease of fabrication, compatibility with large-scale manufacturing, etc.^{34,35} Typically, the microfluidic paper-based analytical devices (μ PADs) can be fabricated using a variety of techniques, such as inkjet printing, wax printing, photolithography, paper cutting, and paper origami. The μ PADs are good candidates for developing POC applications by integrating various functionalized components. Sample handling can be controlled *via* capillary forces through the patterned hydrophobic barriers without the assistance of pumps. Despite the broad applications of μ PADs in diagnostics, environmental monitoring, biomedical and forensic analysis, there are still challenges that must be considered, such as the weak mechanical property, lack of optical transparency, low resolutions of patterned microstructures, ineffective sample consumption (e.g., *via* evaporation), low performance in liquid control, and large variations in specificity and sensitivity.³⁶ Moreover, current colorimetric detection methods have been largely applied to microfluidic paper-based devices, whereas semi-quantitative measurements are still dominant with flawed limits of detection (LODs).

1.2 Polymer and paper hybrid microfluidic devices

These aforementioned limitations of different single-substrate microfluidic systems have motivated the development of hybrid microfluidic systems, particularly cost-effective polymer and paper hybrid microfluidic devices. Hybrid microfluidic systems are meant to adopt the merits of different substrates while avoiding the drawbacks of individual substrates.

The design and fabrication of polymer and paper hybrid microfluidic devices are contingent on assorted requirements and applications.^{3,37} On one hand, extra benefits and more features have been presented in hybrid microfluidic devices, while avoiding certain limitations from individual substrates. For example, the inclusion of paper in a PDMS/glass/paper hybrid device led to the rapid and stable immobilization of aptamers for the multiplexed detection of pathogens and infectious diseases, without complicated surface modification.^{2,38} Another paper/PC/PDMS hybrid device could combine the flexibility of PDMS and the convenience of colorimetric readouts on paper.³⁹ The hybrid device solved the issue of the time-dependent inconsistency in the

conventional test strip, providing an effective and user-friendly platform for rapid and qualitative POC detections. In addition to rapid immobilization of biomarkers in paper/polymer hybrid devices, the integrated device can also increase the efficiency of bioassay *via* analyte enrichment on paper for high-sensitivity multiplex detection of disease biomarkers.^{40,41} On the other hand, hybrid microfluidic systems are competent to integrate many different microstructures and elements to accommodate numerous application requirements. For instance, a PDMS/SU-8 photoresist/glass hybrid device was designed and applied to integrate four label-free detection methods (*i.e.*, impedance, refractive index measurement, optical absorption, and fluorescence), offering a multifactorial analysis tool for complex samples.⁴² Another hydrogel/PMMA/PDMS/glass hybrid microfluidic system was manufactured as a suitable packaging approach for cell culture.⁴³ The system was capable to maintain good surface reactivity, tight sealing, precise control of molecule release, and continuous perfusion cell culture.

Overall, by taking the advantages of various substrates, while eliminating certain limitations of individual chip substrates, polymer and paper hybrid microfluidic devices have been applied in various biological and biomedical applications. Based on the nature of target substances, these applications can be classified into: nucleic acid analysis (including nucleic acid extraction, amplification, and detection), protein analysis (such as the detection of protein-based biomarkers), whole-cell analysis (mostly pathogenic cells), 3D cell culture (allowing cell growth in a 3D model), organ-on-a-chip, and tissue engineering (allowing cell co-culture and mimicking the microenvironment of the natural organs and tissues).

Although numerous successful polymer and paper hybrid microfluidic devices and applications have been reported until now, very limited resources can be approached to summarize their recent advances. In this review, the aim is to: i) review current advances in the design and fabrication of polymer and paper hybrid microfluidic devices; ii) summarize the versatile applications of these hybrid microfluidic devices; iii) highlight unique benefits from such hybrid microfluidic devices. We focus on recent innovations in cost-effective polymer and paper hybrid microfluidic devices. Based on different dominant materials, these hybrid microfluidic devices have been categorized into four types: PDMS-based hybrid microfluidic systems (section 2), thermoplastics-based hybrid microfluidic systems (section 3), paper/polymer hybrid microfluidic systems (section 4), and other emerging hybrid microfluidic systems (section 5). In subsequent sections, we will first briefly introduce each type of hybrid microfluidic devices and their relevant fabrication methods, and then review current biological and biomedical applications of such hybrid devices, including human health diagnostics, cell culture, organ-on-a-chip, and tissue engineering. At the end of this article, we will discuss the current status and future perspectives.

2. PDMS-based hybrid microfluidic systems

PDMS has been widely selected in the fabrication of microfluidic devices with numerous benefits over glass and silicon. First, the prepolymers and curing agents to make PDMS are inexpensive and commercially available. PDMS can be fabricated easily and further processed under ambient conditions without the need for cleanroom facilities. Hence, the cost of the fabrication of PDMS-based devices has been significantly decreased. Second, PDMS, as a flexible material, allows easy and rapid prototyping as well as manipulation *via* polymerization and cross-linking reactions. Third, PDMS is impermeable to water while having high gas permeability, which allows separations between hydrophobic contaminants from water and free exchange of oxygen and carbon dioxide, especially in cell culture.⁴⁴ Fourth, PDMS can be easily assembled to itself and other flat substrates reversibly *via* van der Waals forces or irreversibly after plasma treatment. The hydrophobic surface of PDMS can be easily modified to be hydrophilic by exposure to an air plasma. In addition, the optical transparency of PDMS makes it compatible with many optical detection methods.

To meet the growing requirements of microfluidic devices for biological studies, PDMS-based hybrid devices have been promoted to avoid the limitations of PDMS-only devices, such as low tolerance for high temperature and pressures, poor cell adhesion, nonspecific adsorption of small molecules, and swelling or shrinking in the presence of most organic solvents. Several materials such as glass, thermoplastics, and cellulose (such as filter paper and chromatography paper), have been chosen to incorporate with PDMS, forming different PDMS-based hybrid devices.

2.1 Fabrication

Several technologies based on soft lithography have been employed to manipulate the elastomeric structures on PDMS-based hybrid devices,^{45,46} such as rapid prototyping, replica molding, capillary molding, microcontact printing, and microtransfer molding, although there are some other methods including injection molding and laser ablation.⁴⁶ During general procedures of soft lithography, a liquid mixture of PDMS prepolymers and curing agents is mixed thoroughly and degassed in vacuum to remove air bubbles. The PDMS layers are then cast by pouring the above mixture over a patterned master, followed by thermal curing (*e.g.*, 70 °C) and simply peeling off the PDMS membranes.

The fabrication of PDMS hybrid devices relies on the assembly and sealing of PDMS layers with other hybrid materials. Thanks to its unique flexible property, PDMS can be either assembled to itself or other flat substrates reversibly or sealed irreversibly after plasma treatment of both substrates. PDMS/glass hybrid devices are developed, in which glass slides can act as support substrates with irreversible sealing based on the covalent bonds of Si–O–Si

between plasma-treated PDMS and glass.³⁸ In addition, glass slides can also work as auxiliary layers to integrate other components like microelectrodes. For instance, a glass wafer was used as a handing layer to fabricate silver nanoparticles-based microelectrodes on PDMS by inject printing.⁴⁷ Similarly, other substrates like various membranes and thermoplastics are also assembled with PDMS to form different PDMS hybrid devices. Given varying fabrication methods in PDMS hybrid devices with different materials, more details will be explained in the following section when introducing individual examples of such devices.

2.2 Applications

PDMS-based hybrid microfluidic systems have been widely used in a broad range of biological and biomedical applications, as summarized in Table 1, including substrates, application targets, and LODs.

2.2.1 Nucleic acid analysis

DNA amplification-based. PCR is the most widely adopted nucleic acid amplification method with wide applications in clinical, biological, and forensic analysis.^{48,49} Typically, independent microfluidic compartments for cell lysis and nucleic acid extraction (e.g., by magnetic microbeads) are required to achieve PCR amplification in a microfluidic system. However, it involves complicated and costly microfabrication of micro-pumps and micro-valves,⁵⁰ and inevitable nucleic acid loss and dilution during the elution and transfer procedures, which lowers the sensitivity of nucleic acid analysis. The emerging hybrid microfluidic systems provide a simple and efficient approach for integration of DNA extraction and amplification. The simply embedded membrane substrate (e.g., aluminium oxide membrane or AOM) serves as a capture phase for DNA extraction and for the subsequent DNA amplification that can be achieved in the same single compartment of a hybrid microfluidic system.

Oblath *et al.*⁵¹ reported an AOM/PDMS microfluidic chip integrated with DNA extraction, amplification, and detection for the identification of bacteria in saliva in 7 parallel wells. Samples of lysed target organisms after heating were added in each microwell and filtered through AOM (with a pore diameter of 200 nm) by using vacuum for DNA extraction, followed by the addition of PCR reagents and thermal cycling for real-time PCR. A saliva sample spiked with 300 fg (100–125 copies) of both methicillin-susceptible and methicillin-resistant *Staphylococcus aureus* (*S. aureus*) was used as a demonstration for identification of *Streptococcus mutans*, exhibiting the capability of the hybrid system for simultaneous identification of multiple target species and strains of bacteria in the same sample. The system could achieve the LOD of as low as 30 fg (8–12 copies) of methicillin-susceptible *S. aureus* genomic DNA in a buffer. Compared with conventional DNA amplification methods, this AOM/PDMS hybrid microfluidic device demonstrates a simple and efficient sample preparation

approach by reducing reagent consumption, transfer steps, processing time, and space requirement.

DNA hybridization-based. To achieve identifications of various bacterial pathogens in a single assay, a PDMS/glass hybrid microfluidic device that combined continuous-flow PCR and DNA hybridization was reported.⁵² The glass substrate in this hybrid microfluidic device provided an immobilization surface for DNA probes. Universal primers targeting the conserved regions of bacterial 16S ribosomal DNA (16S rDNA) from a wide range of bacterial species were designed for PCR amplification, and species-specific probes from a variable region of 16S rDNA were designed for DNA hybridization. After the on-chip continuous-flow PCR in a PDMS amplification unit, amplicons were directly introduced into a hybridization unit and hybridized with specific DNA probes immobilized on an aldehyde-activated glass slide. This hybrid microfluidic device was successfully demonstrated for simultaneous identification of five clinically significant bacterial species within 2.5 hours. The LOD of 74 CFU per assay was achieved for the detection of *Escherichia coli* (*E. coli*).

In order to achieve enhanced reaction kinetics and sensitivity of DNA microarray hybridization, Han *et al.*⁵³ presented a PDMS/glass hybrid microfluidic chip-based isotachophoresis (ITP) method to selectively focus and transport target molecules over the immobilized probe sites of a microarray, which could effectively increase the target concentration and the binding reaction rate. The microfluidic chip consisted of a PDMS layer containing microchannel substructures bonded to a glass slide. The glass surface enabled the immobilization of 60 spots of ssDNA probes in a standard microarray. Using 100 fM target molecules, the hybrid microfluidic chip exhibited an 8.2-fold increase in signal within only 30 min compared to a conventional overnight microarray hybridization method.

2.2.2 Protein analysis. PDMS-based hybrid devices have been extensively used for protein analysis, such as the detection of protein-based cancer biomarker.⁵⁴ Jolly *et al.* performed a dual quantification assay for the detection of cancer biomarkers in a PDMS/glass hybrid device.⁵⁵ A PDMS layer consisting of microchannels was sealed onto a cleaned glass substrate *via* a UV-ozone treatment. Salinization was performed for the immobilization of a DNA aptamer that replaced the primary capture antibody. A secondary antibody and a lectin were used to quantify the amount of free prostate-specific antigen (fPSA) and its glycosylation level by chemiluminescence. The LOD of 0.5 ng mL⁻¹ for fPSA and 3 ng mL⁻¹ for glycosylated fPSA was obtained using the hybrid device. Liu *et al.* also developed an aptamer-based sandwich assay in a PDMS/glass hybrid device based on multivalent aptasensor (MAA) array and silver aggregated amplification (SAA) strategy.⁵⁶ Both the glass and PDMS layers were plasma treated to obtain a hydrophilic surface for immediate spotting of aptamer-modified silver nanoparticles (AgNPs) in an array, followed by injection of the target protein and

Table 1 Summary of PDMS-based and thermoplastic-based hybrid microfluidic systems and their applications

Polymer hybrid microfluidic systems	Applications	Platforms	Application targets	LODs	Ref.
PDMS-based	Nucleic acid analysis	PDMS/AOM	<i>S. aureus</i>	30 fg (8–12 DNA copies)	51
		PDMS/glass	<i>E. coli</i>	74 CFU per assay	52
	Protein analysis	PDMS/glass	Synthetic DNA	—	53
		PDMS/glass	fPSA	0.5 ng mL ⁻¹	55
		PDMS/glass	PDGF-BB	1.4 pg mL ⁻¹	56
		PDMS/glass	CA125, HER2, HE4, eotaxin-1	15, 17, 21, 6.5 fM	59
		PDMS/glass	Apolipoprotein A1	12.5 ng mL ⁻¹	60
	Cellular analysis	PDMS/glass	EGFR	3.03 pg mL ⁻¹	61
		PDMS/PC	Influenza	~10 ⁴ TCID ₅₀ titer per mL	57
		PDMS/PMMA	PSA, PSMA	15, 4.8 fg mL ⁻¹	58
3D cell culture	Cellular analysis	PDMS/glass	<i>Listeria</i> cell	1.6 × 10 ² CFU per mL	45
		PDMS/glass	<i>E. coli</i>	100 cells per mL	64
	3D cell culture	PDMS/PMMA	<i>K. pneumoniae</i> , <i>M. marinum</i>	—	46
		PDMS/Parylene/glass	<i>E. coli</i> , <i>L. monocytogenes</i> , <i>S. enterica</i>	10 cells	65
		PDMS/glass	Human microvascular endothelial (HMVEC) cell	—	70
		PDMS/glass	Human umbilical vascular endothelial (HUVEC) cell	—	71
		PDMS/PMMA	HepG2 cell	—	67
	Organ-on-a-chip, tissue engineering	PDMS/PMMA	HepG2 cell	—	68
		PDMS/PMMA	Human lung epithelial A549 cell	—	69
		PDMS/PMMA/glass	U-251 MG cell	—	73
		PDMS/PC	PC 12 cell	—	72
		PDMS/PC/glass	HepG2 cell	—	80
Thermoplastic-based	Protein analysis	PDMS/collagen gel/glass	PSC cell, PANC-1 cell	—	77
		PDMS/methacrylate macromers	Chinese hamster ovary (CHO-K1) cell	—	79
		PDMS/glass	Gut (Caco-2 cell), liver (HepG2 cell)	—	84
		PDMS/glass	Gut (Caco-2 cell), liver (HepG2 cell)	—	86
		PDMS/PMMA/glass	Gut (Caco-2 cell), liver (HepG2 cell)	—	85
		PDMS/PC/glass	Brain (hCMEC/D3 cell)	—	87
		PMMA/PG	PSA, PSMA, PF-4, IL-6	50, 100, 10, 100 fg mL ⁻¹	88
		Polyester/PS	Era	10 fg mL ⁻¹	94
		Plastic/double-sided adhesive	HIV, EBV, KSHV	10 ² copies per mL	95
		PMMA/PC	Influenza A	0.1 ng mL ⁻¹	96
Pathogenic cell analysis	Pathogenic cell analysis	PMMA/glass	B type lymphoblast cell	—	97
		PS/collagen	HBV	—	89
		PS/PC	<i>Campylobacter jejuni</i>	—	90
		COP/TPE	<i>Listeria</i> monocytogene	10 CFU per mL	91
		PS/acrylic-based polymer (FullCure 720)	Macrophage	—	98
3D cell culture	3D cell culture	PS/ABS	Endothelial cell	—	99
		PS/agarose film	A549 cell, NIH 3T6.7 cell	—	100

Note: “—” means LODs not mentioned or applicable from the reference.

aptamer-modified AgNPs tag for aggregation and amplification of the signal. Platelet-derived growth factor-BB (PDGF-BB) and vascular endothelial growth factor-165 (VEGF-165) were simultaneously detected, and the device showed a

linear range from 16 pg mL⁻¹ to 250 ng mL⁻¹ and LOD of 1.4 pg mL⁻¹ for PDGF-BB.

Along with glass, PMMA and PC are also commonly used in the fabrication of PDMS-based hybrid microfluidic devices

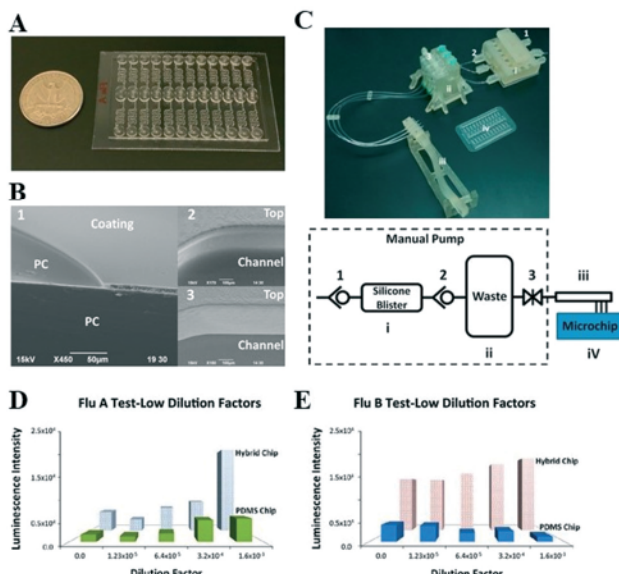


Fig. 1 Protein-based viral analysis using the PC/PDMS hybrid microchip device. (A) A PC/PDMS hybrid microchip for assay of influenza along with a US quarter dollar coin. (B) SEM photos of epoxy sol-gel coating on PC bottom plate (1) and morphology change of PDMS channel surface after (2) and before coating (3). (C) Photo and schematic diagram of a prototype μENIA microchip platform for diagnosis of influenza viruses (i. silicone blister chamber; ii. waste; iii. Handheld pump-to-chip interfacing wand; iv. PC-PDMS hybrid microchip; valves 1–3). (D–E) mENIA of influenza viruses using hybrid and PDMS only microchips. Inactivated influenza strains A/Solomon Island/03/2006 (H1N1) (D) and B/Lee/1940 (E) were used in flu A and flu B antigen assays, respectively. Reprinted with permission from ref. 57. Copyright 2016 Elsevier.

for protein analysis. Liu *et al.* developed an epoxy silica sol-gel functionalized PC/PDMS hybrid device for detection of influenza virus using europium NPs.⁵⁷ The hybrid microchip was fabricated by bonding the patterned PDMS substrate to a piece of pre-cut PC sheet using GPTMS-TEOS sol-gel as a thermal adhesive. The influenza assay results showed that hybrid microchips were superior to native PDMS microchips and a typical commercial laboratory photometric influenza test in terms of assay sensitivity and repeatability (see Fig. 1). The LOD of influenza on the hybrid device was found to be 1.04×10^4 -fold dilution for strain A/Solomon Island/03/2006 (H1N1) and 72-fold dilution for strain B/Lee/1940. Sharafeldin *et al.* developed an electrochemical PDMS/PMMA hybrid device for amperometric detection of cancer biomarkers.⁵⁸ Anti-prostate specific antigen (PSA) and anti-prostate specific membrane antigen (PSMA) on Fe_3O_4 nanoparticles were loaded onto graphene oxide nano-sheets-coated working electrodes (an 8-carbon printed electrode array) as capture antibodies under magnetic control. The detection chamber had a PDMS channel between two symmetrically placed PMMA plates, while the top PMMA layer held a counter Pt electrode and a reference Ag/AgCl electrode. They achieved the LOD of 15 fg mL^{-1} for PSA and 4.8 fg mL^{-1} for PSMA in serum with electrochemical detection.

More components (e.g., semiconductors and microelectrodes) and functions can be incorporated into PDMS-based hybrid microfluidic devices to enhance multiplexing and sensitivity of protein assays. For example, Nguyen *et al.* fabricated a plasmon length-based surface-enhanced Raman scattering (SERS) immunosensor on a PDMS-based hybrid device for panel detection of breast cancer biomarkers.⁵⁹ Glass slides were used as a support for the PDMS/glass hybrid device to build inlet and outlet connections for the SERS immunosensor. The reaction chamber was surface modified through thiol functionalization followed by maleimide-crosslinking for conjugation of antibodies. Cancer antigen (CA125), human epidermal growth factor receptor 2 (HER2), epididymis protein (HE4), and eotaxin-1 were detected in the integrated SERS-microfluidic device from patient-mimicked serum, with LODs of 15 fM , 17 fM , 21 fM , and 6.5 fM , respectively. Lin *et al.* developed a semiconductor embedded PDMS-based hybrid microfluidic chip consisting of four layers of PDMS and a layer of glass substrate coated with 300 nm of aluminum to guide the electrochemical impedance spectroscopy (EIS) electric signal out for the detection of Apolipoprotein A1 using bead-based immunoassays.⁶⁰ Magnetic beads-based immunoassay was used to surpass the issue of protein's distance to sensor surface more than the Debye length. Microvalves and micromixers were used for efficient mixing, reducing the immunoassay time to 1 h and the LOD to 12.5 ng mL^{-1} . Regiart *et al.* reported a PDMS/glass hybrid microfluidic immunosensor using photolithography to pattern a mold for the casting of the PDMS layer containing the microchannels and a glass slide with patterned electrodes (a 20 nm adhesion layer of silver followed by 100 nm of gold) deposited by sputtering. The gold electrodes were coated with CMK-3/poly-acrylamide-co-methacrylate of dihydrolipoic acid nanocomposites for the detection of epidermal growth factor receptor (EGFR) in human serum samples.⁶¹ Anti-EGFR antibody was covalently immobilized on amino-functionalized mesoporous silica (AMS) that was retained in the central channel of the hybrid microfluidic device. EGFR in the human serum sample was detected with the LOD of 3.03 pg mL^{-1} and a linear range of 0.01 ng mL^{-1} to 50 ng mL^{-1} .

2.2.3 Whole-cell detection of microorganisms. In addition to the above applications targeting nucleic acids and proteins, the whole-cell detection, especially for intact microorganisms, using microfluidics has also attracted increasing attention. The direct detection of pathogenic bacterial cells poses advantages in high simplicity by minimizing costly and cumbersome macromolecules isolation procedures.^{62,63} PDMS-based hybrid devices have provided a potential platform for detection of bacterial cells by integrating with other materials such as glass, PMMA, and porous membranes. Typically, glass is used as a sealing layer or support base. Chen *et al.* developed a PDMS/glass hybrid microfluidic device incorporated with biosensors for rapid and sensitive detection of foodborne pathogens, using

Listeria monocytogenes as a model.⁴⁵ The separation and detection chips were fabricated based on 3D printing and soft lithography, in which the PDMS channels and glass slides were bonded after surface plasma treatment. In the fluidic separation chip, glass was used as the support, while a glass wafer with an interdigitated microelectrode was used in the detection chip for impedance measurement. *Listeria* cells, the anti-*Listeria* monoclonal antibodies modified magnetic nanoparticles (MNPs), and the anti-*Listeria* polyclonal antibodies, and urease modified gold nanoparticles (AuNPs) were firstly mixed and incubated in the fluidic separation chip, producing the MNP-*Listeria*-AuNP-urease sandwich complexes. The complexes were then captured in the separation chip by applying a high gradient magnetic field. Through the catalysis of the urease on the complexes, urea used to resuspend the complexes was hydrolyzed into ammonium ions and carbonate ions, and transported into the microfluidic detection chip. The amount of the *Listeria* cells was determined with an interdigitated microelectrode for impedance measurement. The high capture efficiency of cells in the separation chip was achieved up to 93% within 30 min and the LOD of the *Listeria* cells was 1.6×10^2 CFU per mL within 1 h. Another PDMS/glass hybrid device was developed to detect *E. coli* cells.⁶⁴ By modifying PDMS microchannels with 7-polyamidoamine dendrimers and aptamers, the cell capture efficiency increased, achieving sensitive (LOD of 100 cells per mL) and high throughput detection of foodborne pathogenic bacteria.

To achieve more functions on one chip, more than two substrates have also been selected to fabricate the PDMS-based hybrid devices. Delince *et al.* described a PDMS/cellulose membrane/PMMA hybrid microfluidic platform, InfectChip, to study the interactions between pathogenic bacteria and motile eukaryotic phagocytes *via* long-term live-cell microscopy. This platform (Fig. 2A) consisted of a coverslip, cellulose semi-permeable membrane, a PDMS layer, and a PMMA holder.⁴⁶ The coverslip was patterned by coating SU8 on borosilicate wafers using photolithography. The cellulose membrane was clamped between two pieces of filter paper, desiccated for several days, and rehydrated with culturing medium prior to use. Cells were separated from the flow while nutrients could diffuse across the membrane. PDMS layers were fabricated using soft lithography techniques and could be used multiple times. Rapid and reversible medium switches on-chip allowed the continuous flow of medium and thus the real-time analysis of host-pathogen interactions during the long-time cell culture. Motile infected cells were trapped in InfectChip for high-resolution time-lapse microscopy. The direct visualization of all stages of infection was achieved from bacterial uptake to the death of the bacterium or the host cell. By co-culturing a host-cell model, *Dictyostelium discoideum*, with the extracellular pathogen *Klebsiella pneumoniae* (*K. pneumoniae*) or the intracellular pathogen *Mycobacterium marinum* (*M. marinum*), the outcome of such infections proved to be heterogeneous, ranging from abortive infection to death of

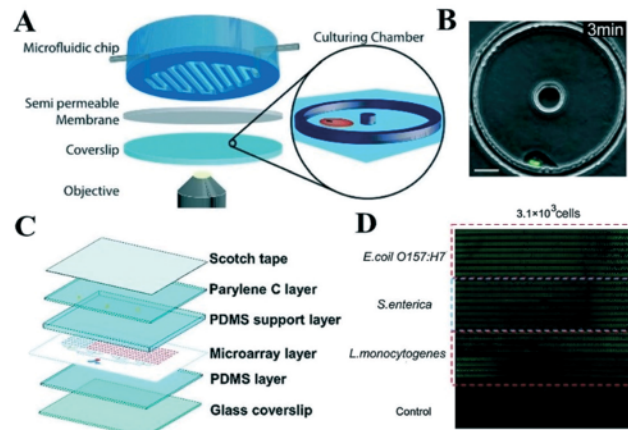


Fig. 2 PDMS-based hybrid microfluidic devices for the cellular detection of microorganisms. (A) Overview of a PDMS/cellulose membrane/PMMA hybrid microfluidic platform, InfectChip. (B) Fluorescence image of *Dictyostelium discoideum* preying on *Klebsiella aerogenes* (green fluorescence), a non-pathogenic strain of the *K. pneumoniae* at 3 min within the InfectChip. Reprinted with permission from ref. 46. Copyright 2016 The Royal Society of Chemistry. (C) Overview of another 6-layer PDMS-based hybrid microfluidic device for multiplexed detection of pathogens. (D) Photographs of foodborne bacteria detected in milk samples with the spiked concentration of 3.1×10^3 cells. Reprinted with permission from ref. 65. Copyright 2020 The Royal Society of Chemistry.

the bacterium or the host cell. For instance, as shown in Fig. 2B, a fluorescence image of *Dictyostelium discoideum* preying on *Klebsiella aerogenes* (green fluorescence), a non-pathogenic strain of the *K. pneumoniae* was obtained, exhibiting that *Dictyostelium discoideum* contacted and internalized the bacteria at 3 min within the InfectChip. By integrating multiple substrates, this InfectChip offered multiple functions including cell separation, culture media refreshing, long-term cell culture, and real-time cellular analysis. Different from the conventional population-based methods, this InfectChip provided a simple and easy method to analyze the time-course of host-microbe interactions at the single-cell level.

Another PDMS/parylene/glass hybrid microfluidic chip was developed by Yin *et al.* and used for rapid, multiplexed detection of foodborne bacteria.⁶⁵ As shown in Fig. 2C, the integrated chip consisted of 6 layers: 3 PDMS layers as a blank layer, a microstructure layer (a microarray layer), and a supporting layer, respectively; a parylene layer to maintain negative pressure; a glass supporting layer; and a tape layer for chip assembly. When applying nucleic acid extraction and integrated multiplex digital recombinase polymerase amplification procedures, the DNA and elution reagents were transported into the microwells due to the negative pressure. Quantitative performance was investigated *via* fluorescence imaging, showing consistent results between the number of positive chambers and the expected copy number from 10 to 2000 copies. The multiplexed detection of three types of foodborne bacteria, *E. coli*, *Listeria monocytogenes* (*L. monocytogenes*), and *Salmonella enterica* (*S. enterica*), was

achieved in spiked milk samples. The results are shown in Fig. 2D, with obvious fluorescence signals when testing samples spiked with 3.1×10^3 cells as compared to control samples, achieving high specificity and the LOD of 10 bacterial cells. The device contained up to 12 800 chambers with only 2.7 nL of reagents in each chamber, and the whole process was completed within 45 min, providing several benefits of high throughput, low sample consumption, rapid detection process, and high sensitivity and specificity.

2.2.4 3D cell culture. Among various reported hybrid devices, PDMS-based hybrid devices have been well developed in 3D cell culture, in which different materials were exploited, such as glass,⁶⁶ PMMA,^{67–69} collagen gel,^{70,71} and PS,⁷² leveraging oxygen permeability of PDMS for cell culture.

Typically, glass has been used as a support base or a cover layer in the PDMS/glass hybrid microfluidic device for 3D cell culture. For example, Zhu *et al.* developed a PDMS/glass hybrid device *via* 3D printing and soft lithography, which was used as a μ -electrotransfection device for 3D cell culture.⁶⁶ PDMS blocks were fabricated to construct the cell culture chamber by using a 3D-printed reusable mold and then assembled with a glass slide as support. Hela cells and Kek-193 cells were seeded on the chip as model cell lines, followed by the 3D electroporation and electrotransfection of cells with the assist of mounted electrodes. This device achieved 3-fold increase of transfection efficiency while maintaining over 85% cell viability compared to conventional 3D cell transfection.

PMMA is one of the most popular materials used in PDMS-based hybrid devices for cell culture. In these devices, PDMS is used to form cell culture chambers, while PMMA is served as a support layer or an oxygen-impermeable material. For example, Mao *et al.* introduced a leaf-templated, microwell-integrated microfluidic chip for high-throughput cell culture.⁶⁷ As shown in Fig. 3A, the chip was fabricated *via* the mold-based microreplication method and 3D printing technology using PDMS and PMMA and assembled, obtaining the leaf-templated microfluidic channels for culture medium. Briefly, two PDMS layers were sandwiched by two layers of PMMA slides to avoid leakage, forming closed spaces acting as a vascular system and cell culture chambers. Water, nutrition, and oxygen were transported to cells in each microwell through the microfluidic channels. High-throughput cell culture was performed on-chip, resulting in uniform and accurate cell seeding for microwell arrays and cell culturing. After two days of perfusion culture, the cells were in high viability and easily formed cellular aggregates, as shown in Fig. 3A. This chip has mimicked the complex microenvironment *in vivo* (e.g., hierarchical structures of blood vessels) and provided a novel platform for high-throughput cell experiments *in vitro*. Another PDMS/PMMA/glass hybrid device was reported for 3D tumor cell culture.⁷³ In this device, PDMS was used to fabricate the cell culture chamber bound to a glass cover slide, while a PMMA sheet was integrated to reduce the oxygen diffusion in the

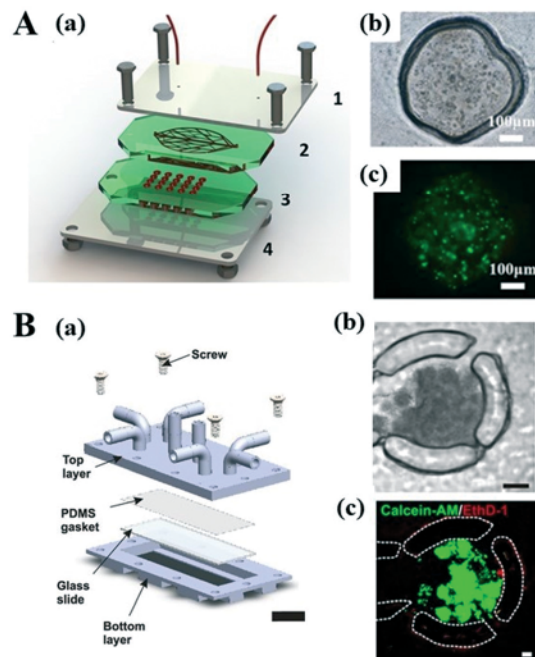


Fig. 3 PDMS-based hybrid devices for 3D cell culture. (A) A PDMS/PMMA hybrid leaf-templated microfluidic chip for high-throughput cell culture. (a) Schematic illustration of the leaf chip, consisting of two PMMA layers (1) and (4), a PDMS layer with leaf-templated microfluidic channels (2), a PDMS layer with microwell arrays (3); (b) phase microscopic image and (c) fluorescent microscopic image of cell stained with live/dead assay growth after two days dynamic culture, respectively. Reprinted with permission from ref. 67. Copyright 2018 IOP Publishing. (B) A 3D printed PDMS/PC hybrid microfluidic spheroid culture system. (a) Exploded view of the device setup. Scale bar = 1 cm; (b) transmission image and (c) fluorescent microscopic image of HepG2 spheroids cells stained with live/dead assay after 72 h of perfusion culture. Scale bar = 100 μ m. Reprinted with permission from ref. 80. Copyright 2017 IOP Publishing.

chamber due to its oxygen impermeability. With different hypoxic conditions, the human glioblastoma astrocytoma U-251 MG cells were cultured using this device to study cell growth variations and metabolic changes under different microenvironments.

In addition, Yajima *et al.* developed a perfusable 3D liver cell cultivation system on a PDMS/microfibers/PMMA hybrid device.⁶⁸ The microfluidic system consisted of cell-laden hydrogel microfibers, PDMS, and PMMA. Two types of PDMS devices were fabricated using soft lithography and replica molding to produce cell-laden microfibers and for perfusion cultivation, respectively. The microfibers were recovered using a roller and tied up to form a fiber bundle. An open-air perfusion chamber packed with the bundle was then sealed with PDMS, followed by being fixed using PMMA plates and stainless-steel jigs. With the Hepatic lobule-like construct, the high-density cell cultivation was approached to evaluate cell viability and functions. This microfluidic system could mimic the hepatic lobule structures *in vivo* and provide a useful platform for biomedical applications.

In some cases, PMMA and PDMS could be pre-mixed to fabricate polymer membranes to be integrated into microfluidic devices. Moghadas *et al.* recently reported a PDMS/PMMA hybrid microfluidic device for on-chip cell culture integrating an electrospun membrane.⁶⁹ The membrane was fabricated with a high ratio of PDMS to PMMA (*i.e.*, 6:1 w/w), which increased the flexibility of the membrane and avoided the leakage. Human lung epithelial cells (A549) were immobilized on the membrane within the hydrophobic micropores with no aid of extracellular matrixes for cell adhesion and cell growth. The continuous flow of the culture medium through microchannels provided a shear-free and *in vivo*-like cell culture condition, with a flow rate of up to 50 $\mu\text{L min}^{-1}$. Different configurations including single cells, monolayer cells, and 3D cell clusters were observed due to the 3D topography of the membrane. By using this pre-mixed PDMS/PMMA strategy, the membrane surface conditions between hydrophobic and hydrophilic can be adjusted easily, and the device could be used to culture anchorage-independent and anchorage-dependent cells, respectively, for other applications such as pharmacodynamics research.

Collagen has been commonly used as an important extracellular matrix (ECM) component in the PDMS-based hybrid systems for 3D cell culture.^{74–76} For instance, Ge and co-workers reported several PDMS/collagen gel/glass microfluidic devices to mimic the *in vivo* microenvironment and studied the effect of VEGF in vascular development, maturation, and angiogenesis.^{70,71} These devices were fabricated from PDMS using soft lithography and mostly assembled with glass slides as support layers through plasma treatment. Collagen gel was introduced through microchannels, followed by cell seeding and culturing, which mimicked the blood vessel wall. The hydrostatic pressure in the inputs was controlled to allow the directional flow of cells through microchannels, which enabled the binding of cells to the gel region and formed the basis for the monolayer of cells. By varying the composition of cellular growth media, different growth factor gradients could be established to stimulate cellular responses and generate agent-based stochastic responses. Lee *et al.* reported a multi-microchannel plate-based PDMS/collagen gel/glass device for 3D culture of pancreatic tumor cells.⁷⁷ The device consisted of PDMS replicas as cell culture chambers, type I collagen to facilitate the cell loading onto the PDMS microchannel surface, and a glass slide as a coverslip. The pancreatic stellate cells (PSCs) and human pancreatic cancer cells (PANC-1) were co-cultured on this device to mimic the epithelial-mesenchymal transition and chemoresistance. Their results showed that the number of PANC-1 cells increased when co-cultured with PSCs, forming 3D tumor spheroids, and the expression of alpha-smooth muscle actin (α -SMA) in PSCs also increased. When exposed to gemcitabine and paclitaxel, the growth of tumor spheroids was inhibited with significant cytotoxicity of PSCs. This work provided a promising platform to study cell-cell, cell-ECM, and cancer cell-PSC interactions, as well as drug responses.

PS has also been applied to design PDMS-based hybrid devices for cell culture due to its ease of integration with electrodes and biological compatibility.^{72,78} Johnson *et al.* fabricated a PDMS/PS hybrid device to monitor the neurotransmitter release from PC 12 cells.⁷² This hybrid device combined the advantages of PDMS to incorporate pumps and valves, with the ability of PS to easily embed electrodes for cellular analysis and tubing to provide a low dead-volume interface for off-chip sampling. The surface was treated using chlorotrimethylsilane to obtain the robust and reversible sealing between PS and PDMS substrates. Cell releasate was first withdrawn continuously from the cell culture dish through the embedded capillary and onto the microchip. The analytes, dopamine (DA) and norepinephrine (NE) were then electrophoretically separated and detected amperometrically using PS-embedded electrodes. The concentrations of DA and NE were detected to be $29 \pm 2 \mu\text{M}$ and $31 \pm 2 \mu\text{M}$, respectively, when cells were stimulated with K^+ . Incorporation of multiple processes was achieved on the hybrid device involving continuous sampling from off-chip cell culture, on-chip electrophoresis, and electrochemical detection. However, an improvement can be expected to integrate on-chip cell culture on hybrid chips.

More recently, an automated digital manufacturing process to fabricate PDMS-based hybrid devices for cell culture can be achieved by integrating 3D printing technology, such as stereolithography. Bhattacharjee *et al.* developed a 3D-printable microdevice for mammalian cell culture, which utilized commercially available PDMS-methacrylate macromers (a high-efficiency photoinitiator and a high absorbance photosensitizer) based on stereolithography.⁷⁹ The 3D-printable PDMS resin (3DP-PDMS) was formulated to have high efficiency of photopolymerization with 385 nm UV light. Properties remained similar to that of the conventional thermally cured PDMS (Sylgard-184), such as optically transparent, gas-permeable, highly elastic, and biocompatible, whereas the automation of manufacturing processes was improved due to the 3D printing technology. Prior to the on-chip cell culture, the toxic photopolymerization byproducts and unreacted compounds were extracted from the devices to make them cytocompatible. In their comparative studies of cell culture on the control molded-PDMS, extracted, and unextracted devices, the results proved that the extracted device using hybrid materials could support long-term growth, proliferation, and viability of mammalian cells.

Another 3D printed PDMS/PC/glass microfluidic device was reported by Ong *et al.* for multicellular spheroid perfusion cultures.⁸⁰ Fabricated by the stereolithography technology, the device contained a 3D printed top layer using a PC layer and a bottom mounting base. As shown in Fig. 3B, the top layer included a cell culture chamber, perfusion and seeding channels, and connecting Luer interfaces, while the bottom base integrated with PDMS as a gasket due to its intrinsic elastomer and proper sealing property, and a glass slide as an optical window due to its optical transparency. All

parts were assembled with steel screws and the device implemented pump-free perfusion based on gravity-driven flow, reducing complexity. The perfusion cultures of patient-derived parental and metastatic oral squamous cell carcinoma tumor and liver cell (HepG2) spheroids were performed on the device, showing good cell viability and functionality for up to 72 h.

2.2.5 Organ-on-a-chip and tissue engineering. Microfluidic technologies provide more physiologically relevant environments (such as extracellular microenvironments) than those in conventional cell culture experiments, which can recapitulate the tissue architecture and functional complexity of living organs by precisely controlling cell localization and cultivation.^{81,82} PDMS is among the most widely used microchip materials in the applications of organ-on-a-chip and tissue engineering. Hybrid microfluidic devices are well-suited for the application in organ-on-a-chip since different compartments with specific target organ functions can be integrated into one chip using various materials.⁸³ PDMS-based hybrid microfluidic devices are dominant in this field.

Sung's lab presented several PDMS-based hybrid devices for gut-liver-on-a-chip applications. For example, a microfluidic gut-liver chip was fabricated based on soft lithography using PDMS, a polyester membrane, and a glass slide.⁸⁴ The porous polyester membrane as a cell layer was assembled on PDMS and then bonded with glass slides as a support base, fabricating a PDMS/polyester membrane chip/glass hybrid device to reproduce the dynamics of the first pass metabolism. The chip contained two separate layers for gut epithelial cells (Caco-2) and the liver cells (HepG2). These two different cell lines could be co-cultured on-chip to record the physiological function of both cells. Apigenin, as a model drug, could go through a sequential absorption in the gut chamber and a metabolic reaction in the liver chamber. The metabolic profile was proved to be closer than that with a monoculture of gut cells. This microfluidic gut-liver chip provides a potential platform to evaluate the first pass metabolism of drugs *in vitro*. A more complicated microfluidic gut-liver culture chip was fabricated containing five PDMS layers, a glass slide, a porous membrane, and two PMMA layers.⁸⁵ The top and bottom PMMA layers and PDMS layers were assembled using screws, while the glass slide and PDMS layers were bonded with the treatment of air plasma. All compartments and fluidic channels were fabricated on PDMS layers with transwell inserts containing a porous membrane, which allowed cells seeding and culturing. Both 2D and 3D cell co-culture of gut and liver cells could be achieved on the microfluidic system. By using this device, it was possible to reproduce the first pass metabolism of oral drugs based on pharmacokinetic (PK) profiles. Besides drugs, the gut-liver chip was also employed to mimick the absorption and accumulation of fatty acids.⁸⁶ Two separate flows were introduced to represent the food ingestion and the blood flow. Perfusion flow was achieved by using gravity-driven flow on the chip. The absorption of fatty acids in the gut and accumulation in the liver was accomplished on the

single hybrid chip, working as an *in vitro* model of hepatic steatosis.

Several PDMS/PC hybrid systems have been developed for organ-on-a-chip. For instance, Helm *et al.* established an organ-on-chip system to directly quantify transendothelial electrical resistance (TEER), as well as monitoring cellular barrier tightness.⁸⁷ The chip was prepared from PDMS, PC membrane, and glass slides. Four electrodes were inserted into microchannels with a sufficiently large surface area to the culture medium. By mimicking the blood-brain using this device, the TEER of a monolayer of human hCMEC/D3 cerebral endothelial cells was quantified directly. The measurements provide accurate and stable readouts, which is benefited from the independence changes in nonbiological factors.

3. Thermoplastic-based hybrid microfluidic systems

Thermoplastics have attracted increasing attention in the fabrication of microfluidic devices, due to the low cost, excellent bio-inertness, simple fabrication, low intrinsic fluorescence, and good compatibility with mass production infrastructures. There are several commercially available thermoplastics including PMMA,⁸⁸ PS,^{89,90} PC,⁹⁰ cyclic olefin copolymer (COC),⁹¹ etc. Among these materials, PMMA has been widely used in hybrid microfluidic systems, whereas it is mostly incorporated with PDMS, as described in section 2. Hence, this section will focus on other thermoplastic materials-based hybrid devices for biological applications, like PS, PC, and COC.

3.1 Fabrication

A variety of methods to fabricate thermoplastic-based hybrid devices have been summarized previously, including direct techniques, such as laser ablation and soft lithography, and replication techniques, such as injection molding, compression molding, and hot embossing.⁹² For instance, during laser ablation, a beam of the high-energy laser is applied to break bonds between polymer molecules and cause photoablation, thus directly engraving thermoplastics based on designed patterns. By precisely controlling the laser position, laser power, and scanning speed, different shape and size can be attained in engraved thermoplastics.⁹³

3.2 Applications

Thermoplastic-based hybrid microfluidic devices have been employed in numerous biological applications, such as protein analysis, pathogenic cellular analysis, and 3D cell culture. Recent applications based on thermoplastic-based hybrid devices are presented as follows and also summarized in Table 1, including the fabrication substrates, targets, LODs, etc.

3.2.1 Protein analysis. Detection of various protein biomarkers for cancer and viral detection has been the major

application of the thermoplastic-based hybrid devices in protein analysis. A few thermoplastics-based hybrid devices were reported involving PMMA and polyester, which are low-cost and can be fabricated easily. Kadimisetty *et al.* fabricated an automated, microprocessor-controlled multiplexed immunoassay device with a 30-microwell detection array and a six-channel system driven by integrated micropumps.⁸⁸ The pyrolytic graphite (PG)/PMMA hybrid detection chip housed with a steel metal shim counter electrode and a Ag/AgCl reference electrode was used for the electrochemiluminescent measurement of four biomarkers, PSA, PSMA, platelet factor-4 (PF-4), and interleukin-6 (IL-6) within 36 min, with the LODs from 10 to 100 fg mL⁻¹. Uliana *et al.* developed a polyester/polystyrene microfluidic electrochemical device where electrodes were modified with DNA sequences known as estrogen response elements for the detection of breast cancer biomarker, estrogen receptor alpha (ER α), with the LOD of 10 fg mL⁻¹.⁹⁴ Electrodes were constructed on polyester sheets using a simple procedure based on the use of a cutter printer for rapid prototyping and vinyl sheets as a negative mask. Polyester sheets with screen-printed electrodes were sandwiched using a double-sided adhesive polystyrene card to develop a fully disposable microfluidic device. Similarly, Shafiee *et al.* also used a plastic/double-sided adhesive hybrid device with printed electrodes for the electrical sensing of viruses.⁹⁵ The hybrid chip was simple and mass-producible as microelectrodes were printed on flexible plastic substrates using conductive inks. The device was applied to evaluate human immunodeficiency virus (HIV), Epstein–Barr virus (EBV), and Kaposi's sarcoma-associated herpes virus (KSHV) at clinically relevant virus concentrations. In addition, Kim *et al.* developed PMMA/PC hybrid microfluidic immunoassay using simple fluid vent control.⁹⁶ A PMMA plate with channels was bonded with a polycarbonate substrate through acetone injection bonding using a customized press machine. The components of this fluorescence-based immunoassay were successfully pre-loaded in the microfluidic device (Fig. 4). The analyte H1N1 Influenza A reacted with the detection antibody conjugated on fluorescence beads, and bound to the capture antibody immobilized zone during channel flow. The pausing of the fluid provided sufficient time for the immune reaction; however, the detection sensitivity was slightly worse than the conventional sandwich fluorescence immunoassay (SFIA) method.

In addition to diagnosis, thermoplastic based hybrid devices have also been used to monitor the treatment of patients. A PMMA/glass hybrid microfluidic device that consisted of four layers for screening the response to leukemia treatment was developed by İçöz and co-workers.⁹⁷ The bottom glass cover was a standard microscope slide; the micro-size gold pads were fabricated on glass wafer using standard lithography and then functionalized with antibodies to capture target cells, while the middle channel layer and top cover were PMMA. The platform was optimized with cultured B type lymphoblast cells and tested with samples of

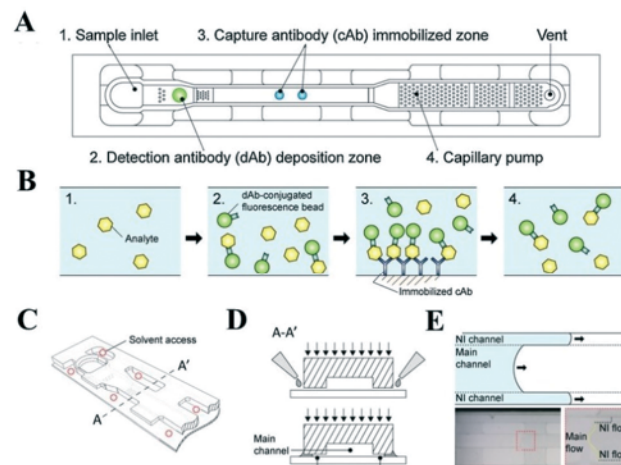


Fig. 4 PMMA hybrid microfluidic devices for immunoassays of viral proteins. Schematic illustration of (A) the microfluidic device comprising immunoassay elements and (B) interaction between antibodies and analytes along the sample flow. (C) Structure of solvent access for the assembled device. (D) Cross-sectional view of the nanointerstice (NI) channel generated by solvent bonding PMMA/PC. The upper plate was made of PMMA while the lower plate was PC. (E) The air-liquid interface (ALI) in channel filling flow. Scale bar, 3 mm. Reprinted with permission from ref. 96. Copyright 2020 Elsevier.

leukemia patients. It exhibited 99% statistical agreement with flow cytometry.

3.2.2 Whole-cell detection of microorganisms. In addition to PMMA, PS-based hybrid microfluidic devices have also been reported for pathogenic cell analysis. Ortega-Prieto *et al.* used a microfluidic primary human hepatocyte (PHH) system to study HBV (hepatitis B) infection.⁸⁹ This system integrated collagen-coated PS scaffolds seeded with PHH for cell adherence and a perfused bioreactor for cell culture media recirculation, which could maintain for at least 40 days. In this method, the recapitulation of all steps of the HBV life cycle could be achieved, involving the replication of patient-derived HBV and the maintenance of HBV covalently closed circular DNA. The results showed that innate immune and cytokine responses following infection with HBV mimic those observed in HBV-infected patients, which was important to study the pathways for immune evasion and validation of biomarkers. In addition, by co-culturing PHH with other non-parenchymal cells, the identification of the cellular origin of immune effectors could be obtained and provided a valuable preclinical platform for HBV research.

PS was also hybridized with PC to fabricate hybrid microfluidic devices. For instance, a PS/PC hybrid microfluidic device was presented by Mortensen *et al.* to culture Caco-2 cells and study the biochemical responses to the bacterial pathogen *Campylobacter jejuni* based on metabolomics analysis.⁹⁰ A 100 mm PC membrane with 0.4 μ m pores was sandwiched between apical and basolateral PS microchannels and the resulting microfluidic device was connected to silicon tubing, a peristaltic pump, and glass vials containing growth media. The membrane was pre-

coated with matrix proteins and collagen to increase cell attachment. By culturing Caco-2 cells on-chip, uniform and defined brush borders, tight junctions, and mucin layers were obtained, allowing for the study of host-pathogen interactions. Metabolomics analysis proved that the microfluidic cell culture had a more homogenous metabolism, and the aminoacyl-tRNA biosynthesis in both mitochondria and cytoplasm of the cells was influenced by the fluid dynamics. It brought out the potential application of combining microfluidic and metabolomics analysis in the studies of infectious diseases.

Cyclic olefin polymer (COP) as a relatively new class of thermoplastic material has been exploited in recent hybrid microfluidic devices because of excellent optical and mechanical properties, great biocompatibility, and high heat resistance. For example, a COP/TPE (cyclic olefin polymer/thermoplastic elastomer) hybrid microfluidic device was reported by Malic *et al.*, which was used for immunomagnetic capture and release of *L. monocytogenes*.⁹¹ A 3D magnetic capture region was made from cylindrical pillars embossed in thermoplastic polymer TPE and soft ferromagnetic nickel coating, thus generating strong and switchable magnetic capture regions and promoting efficient capture of bacteria cells. The efficient localized capture and rapid release of magnetic nanoparticles and immunomagnetic nanoparticles (IMNPs) conjugated to *L. monocytogenes* were achieved within the capture regions. The recovery rate for MNPs and the capture efficiency for live bacteria were up to 91% and 30%, respectively, with the LOD of 10 CFU per mL.

3.2.3 3D cell culture. Several PS-based hybrid devices have been explored for 3D cell culture, usually containing fibers and coated films. For instance, Chen *et al.* presented a scalable and reusable microfluidic device for 3D cell culture, which integrated removable fibrous-immobilized PS inserts with a 3D-printed fluidic device.⁹⁸ The silk fibroin fibers as the ECM analog were extracted from crude silk and collected on the PS sheet *via* electrospinning to culture macrophages, while PS was applied as the fibrous scaffold for cell immobilization. The obtained fibrous sheet was cut using a laser cutter to form inserts. The fluidic device was fabricated using a 3D printer and had customized-designed locking slots along the channels for inserts. The coated inserts were used to culture macrophages, which was found to be polarized to the M1 state (pro-inflammatory state) by lipopolysaccharide (LPS) in a more *in vivo* like manner, compared to those cultured on flat surfaces. Different stimulus immune responses of macrophages were observed, and cytokines quantitation were obtained in the activated M1 state by using this device. In a similar manner, the electrospun PS fibers were integrated with the ABS (acrylonitrile butadiene styrene, as the 3D printing material)-based microfluidic device, acting as a scaffold for endothelial cell culture in the nature-mimicking 3D *in vivo* environment.⁹⁹ The obtained system contained different modules including cell culture, sample injection, and

electrochemical detection of nitric oxide released from endothelial cells, which provided a customized and modifiable microfluidic system for biological studies.

Similarly, Jeong *et al.* developed an agarose film coated-PS microfluidic chips for capture, recovery, and culture of cancer cells, namely, A549 and NIH 3T6.7 cells.¹⁰⁰ The PS chip was prepared by an injection molding process and then treated with oxygen plasma. The agarose film was coated on the PS chip to protect the cell attachment and allow 3D growth of cancer cells, and further modified to covalently or non-permanently bind the photoactivatable Fc-specific antibody-binding proteins. Target cells were then captured on the antibody-modified chips avoiding nonspecific binding and could be readily recovered by the treatment of trypsin-ethylenediaminetetraacetic acid (EDTA) solution. Moreover, it was proven that the captured cells were captured on the micropost walls of chips instead of on the bottom.

4. Paper/polymer hybrid microfluidic systems

In addition to polymer/polymer hybrid microfluidic devices, paper/polymer hybrid devices have also been extensively studied in recent years for low-cost biological and biomedical applications. The paper substrate as an emerging material has attracted increasing attention in the fabrication of microfluidic devices due to many advantages.¹⁰¹ First of all, the paper is ubiquitously available at low cost and with good recyclability and competency as an ideal substrate for many biomedical applications such as POC testing in low-resource settings. Paper is lightweight but it possesses a 3D porous structure, allowing its ease to use for reagent storage and compatibility with the 3D design. Paper can drive the fluid flow owing to the capillary effect, without the need for external pumps. In addition, paper is composed of cellulose or the cellulose-polymer blend, which is compatible with numerous biological samples. Besides, paper can be easily modified to obtain a wide variety of functional groups for binding with biological molecules like protein and DNA. Moreover, the white color of the native paper provides a strong contrast to other colored substrates, making it a good candidate for colorimetric assays.^{101–103}

Despite numerous advantages of paper-based microfluidic devices as a low-cost platform, there are still many issues that paper-based microfluidic devices are faced with. For instance, sample nonspecific adsorption and sample evaporation happen in μ PADs. The patterned hydrophobic barriers in μ PADs may not stay long enough during the long-time sample handling. There is lack of high performance of paper when manipulating liquid fluids. Paper is not well-suited for optical, absorbance, or fluorescence measurement due to its intrinsic opacity, significant light-scattering, and autofluorescence. These limitations have motivated the exploration of paper/polymer hybrid microfluidic devices, which have been developed as advanced platforms for biological applications.^{38,103} The Li group has pioneered this

concept of paper/polymer hybrid devices since 2013.^{2,3,9,14,15,38,41,93,104-109}

4.1 Fabrication

Similar to μ PADs, the fabrication of paper/polymer hybrid microfluidic devices can be initiated by the formation of hydrophobic barriers on paper substrates. Different technologies have been summarized previously include photolithography, wax printing, etching, and cutting.^{92,110-114} For example, in wax printing technology, the wax is printed on the surface of the paper and subsequently melted by baking the paper on a hot plate (e.g., 120 °C). The melted wax will permeate through the paper layer and become solidified in the paper, resulting in the hydrophobic barrier.

Paper is often inserted or embedded into polymeric regions, enabling a simple way for the formation of paper/polymer hybrid devices. Furthermore, some additional processes must be considered, when incorporating with other materials in paper/polymer hybrid microfluidic devices, such as patterning, bonding, embedding, and sealing. Recently, Xu's group presented a new method to fabricate paper/polymer microfluidic devices. A benchtop technique was reported to fabricate 3D reconfigurable hybrid microfluidic devices made from soft paper and polymer composites.¹¹⁵ By simply bending and stretching without the requirement of specialized equipment involved in lithography, this fabrication approach could be completed within 2 hours and produce microchannels with a width of 100 μ m. The fabricated paper/polymer hybrid microfluidic devices were demonstrated using a droplet generator and a reconfigurable electronic circuit.

4.2 Applications

Numerous paper/polymer hybrid microfluidic devices have been developed for a broad range of applications from nucleic acid analysis to 3D cell culture, as summarized in Table 2 including microfabrication materials, application targets, LODs, etc.

4.2.1 Nucleic acid analysis

Integration of nucleic acid extraction and PCR. Filter paper has been used as an optimal substrate in hybrid microfluidic chips for nucleic acid extraction since it is low cost, easy to fabricate, and capable of providing an inhibitor-free nucleic acid template from a variety of raw samples with high extraction efficiency. For instance, Tang *et al.*¹¹⁶ developed a paper/photopolymer resin hybrid microfluidic device for one-step DNA extraction from diverse biological samples. The device was printed with a 3D printer. This device incorporated a sponge-based reservoir module for buffer storage and a paper-based valve and channels for the introduction and fluid path of samples and reagents and a Fusion 5 filter paper disk for DNA capturing. By using only 30 μ L starting samples of whole blood, serum, breast cancer cell, saliva, sputum, and bacterial suspension, DNA could be rapidly extracted within 2 min. The extracted HBV nucleic

acids from clinical blood samples were applied to conventional real-time PCR assays and the LOD of 10⁴ copies per mL was achieved. The DNA extraction performance achieved by this paper hybrid microfluidic device was comparable to that of the commercial QIAGEN DNA extraction kit. However, on-chip PCR amplification was not integrated into this system.

Liu's group developed a filter paper/PDMS/PMMA hybrid microfluidic chip with a Fusion 5 filter paper fabricated in the DNA extraction chamber for DNA extraction from various raw samples and the subsequent on-chip or off-chip PCR amplification.¹¹⁷ The DNA extraction efficiency of the hybrid chip was investigated using human whole blood samples. It was found that 5.6–21.8 ng of DNA was yielded from 0.25–1 μ L of human whole blood samples within 7 min by sequentially aspirating NaOH, HCl, and water through the filter paper (particle retention size of 2.3 μ m), which was higher than those obtained using commercially available QIAamp DNA Micro kits (3.6–13.0 ng). In addition, real-world samples including dried blood stains, buccal swabs, saliva, and cigarette butts were successfully processed for DNA extraction in this hybrid chip as well. This filter paper-based hybrid microfluidic chip was versatile for both off-chip and on-chip amplifications after nucleic acid extraction. By using the filter paper-based extracted DNA from whole blood samples, off-chip PCR amplification of 15-plex short tandem repeat loci and Sanger-based DNA sequencing of the 520 bp GJB2 gene were accomplished. Additionally, on-chip PCR amplification following DNA purification from blood and bloodstains without elution was performed in the DNA extraction chamber, which exhibited the capability of integrating DNA extraction process with downstream PCR amplification in the hybrid chip for nucleic acid analysis.

Liu *et al.*¹¹⁸ developed another filter paper/polymer hybrid microfluidic chip that consists of DNA extraction and PCR and demonstrated the application of the hybrid microfluidic biochip for genetic testing of hereditary hearing loss from human whole blood. In this microfluidic chip, a piece of Fusion 5 filter paper was embedded in a 15 μ L chamber for genomic DNA extraction, followed by on-chip PCR amplification without elution in the same single reaction chamber. Genomic DNA extractions from as low as 0.3- μ L human whole blood was performed, following by PCR amplification for 59-bp β -actin fragments without observing any contamination or carryover problems. The detection of c.176_191del16, c.235delC, and c.299_300delAT mutations in GJB2 gene that related to the hereditary hearing loss was completed within 2 hours by performing the DNA extraction and a two-color multiplex allele-specific PCR assay with the assistance of electrophoretic analysis. All the generic mutations from blood samples donated by a healthy person and five persons with genetic mutations were accurately analyzed.

The Fusion 5 filter paper can be modified by chitosan to improve the DNA extraction efficiency of the hybrid microfluidic chip.¹¹⁹ In this way, the mechanism of the

Table 2 Summary of paper/polymer and other emerging hybrid microfluidic systems and their applications

Paper hybrid microfluidic systems	Applications	Platforms	Application targets	LODs	Ref.
Paper/polymer	Nucleic acid analysis	Paper/photopolymer resin	HBV	—	116
		Paper/PDMS/PMMA	Human genomic DNA, mutations in GJB2 gene	—	117
		Paper/chitosan polymer	Human genomic DNA, bacteriophage λ -DNA	—	119
		Paper/PMMA	<i>N. meningitidis</i> , <i>S. pneumoniae</i>	6–12 DNA copies	2
		Paper/PMMA	<i>Anopheles gambiae</i> and <i>anopheles arabiensis</i> DNA	—	123
		Paper/PDMS	<i>N. meningitidis</i> , <i>S. pneumoniae</i> , Hib	3–12 DNA copies	14, 15
		Paper/PDMS	<i>B. Pertussis</i>	5 DNA copies	106, 125
		Paper/PDMS/glass	<i>S. aureus</i> , <i>Vibrio parahaemolyticus</i>	21.5, 20.9 copies per μL	126
		Paper	<i>Malaria</i>	—	124
		Nitrocellulose/PET/PMMA	T7 bacteriophage	—	129
	Protein analysis	Paper/plastic	Dengue NS1	84.66 ng mL^{-1}	130
		Paper/plastic	CEA/AFP	100 ng mL^{-1}	132
		Paper/polymer	<i>E. coli</i>	10^5 CFU per mL	131
		Nitrocellulose/PDMS	Vaccinia virus protein	—	134
		Paper/PC/PDMS	Proteinuria, glucose, pH, RBC	—	39
Others	Pathogenic cell analysis	Paper/PMMA	IgG, HBsAg	$1.6, 1.3 \text{ ng mL}^{-1}$	40
		Paper/lamination sheet	Hp	$0.73 \mu\text{g mL}^{-1}$	103
		Paper/polyester	Total serum protein, HSA, cocaine, TNT, iron content	0.1 mg mL^{-1} (cocaine)	135
		Paper/PDMS/glass	<i>L. acidophilus</i> , <i>S. aureus</i> , <i>S. enterica</i>	11.0, 61.0, 800 CFU per mL	38
		Paper/PDMS	<i>S. aureus</i> , <i>E. coli</i> , <i>E. faecalis</i>	—	136
	3D cell culture	Paper/glass	NPC cancer cell	—	137
		Paper/glass	Huh7 cell, HepG2 cell	—	138
		Paper/PMMA	Huh7 cell, HepG2 cell, BM-1 cell	—	139
		Paper/PDMS/PMMA	Hela cervical cancer cell	—	140
		Paper/tape	HPV DNA	—	142
Others	Nucleic acid analysis	Paper/microcapillary	CYP2C19 gene	—	143
		Paper/cotton	BSA, urobilinogen, UA, nitrite	$3.672, 4.861, 125.625 \mu\text{M}$, 0.147 mM	144
		Paper/cotton thread/glass fiber	CEA	2.32 ng mL^{-1}	145
		Cotton	Human ferritin	10 ng mL^{-1}	146
		Cotton/polyester	BSA, nitrite, nickel ion	—	147

Note: “—” means LODs not mentioned or applicable from the reference.

chitosan-modified filter paper for DNA capture combined both the physical entanglement of DNA molecules with the fiber matrix of the filter paper and the electrostatic adsorption of DNA molecules to the chitosan polymer. The high capture efficiencies of 98% and 95% for K562 human genomic DNA and bacteriophage λ -DNA were reported respectively.¹¹⁹ In addition, the λ -DNA from a diluted sample with a concentration of $0.05 \text{ ng } \mu\text{L}^{-1}$ could be enriched by a concentration factor of above 30 folds.¹¹⁹ The on-chip DNA extraction coupled with on-chip PCR amplification of 15-plex short tandem repeat loci from blood samples was successfully demonstrated.

Integration of nucleic acid extraction and LAMP. Despite the development of simplified and integrated nucleic acid

extraction processes in various hybrid microfluidic devices, the essential thermal cycles increase the complexity and cost for the microfabrication of the heater and the temperature sensor on a microfluidic system to perform on-chip PCR. In addition, additional off-chip detection approaches such as gel electrophoresis are usually needed to assist the detection. As a promising isothermal nucleic acid amplification method, loop-mediated isothermal amplification (LAMP) has been developed to amplify the target DNA at a constant temperature in a range of 60–65 °C. The high strand displacement activity from a DNA polymerase (e.g., *Bacillus stearothermophilus*, *Bst*) and identification of 6 distinct regions from 4 different primers in LAMP result in high specificity. It has been reported that LAMP has higher

specificity and sensitivity, and less inhibiting effect to clinical samples such as blood than PCR.^{120,121} In addition, LAMP allows nucleic acid amplification to be performed under thermally constant conditions, eliminating the complicated and costly microfabrication of heating elements on a microfluidic chip. The endpoint colorimetric or fluorescent detection can be easily achieved without requiring additional time-consuming and complicated detection approaches or the use of bulky instruments. Thus, the complete “sample-to-answer/read-out” hybrid microfluidic systems can be achieved by integrating sample preparation and LAMP.

Considering a relatively large volume of plasma is required to achieve the high-sensitivity detection for low-abundance target molecules, a low-cost, pump- and centrifuge-free polysulfone membrane/PMMA hybrid plasma separation device was developed to separate plasma from undiluted milliliter whole blood prior to the FTA membrane-based nucleic acid extraction.¹²² The functional plasma separation chamber of the device was composed of an asymmetric and porous polysulfone membrane and the PMMA base for structural support. Both the size exclusion-based membrane filtration and the gravitational sedimentation of blood cells were involved in the separation mechanism. This device could consistently separate $275 \pm 33.5 \mu\text{L}$ of plasma from 1.8 mL of undiluted whole blood within 7 min. By separating plasma laden with HIV viruses from HIV virus-spiked whole blood, high recovery efficiencies of >80% for viral loads of 350–35 000 copies per mL was demonstrated. The separated HIV-laden plasma was then injected into their previously developed FTA paper/PMMA hybrid microfluidic device¹²³ for nucleic acid extraction and reverse-transcriptase LAMP reactions, indicating the plasma separation device could successfully provide sufficient plasma for nucleic acid amplification without inhibitory factors, achieving sensitive detection of low-abundance target molecules from whole blood samples. Reboud *et al.* reported a paper-based microfluidic technology that combines sample processing, DNA isothermal amplification detection for diagnostics of malaria in low resource underserved rural communities.¹²⁴ The microfluidic system included a foldable paper strip for vertical flow-based DNA extraction from whole-blood samples, a plastic cartridge for LAMP reaction, and a lateral-flow paper strip for visualization DNA detection. The tests were performed in village schools in Uganda, and the diagnosis of malaria species from a finger prick of whole blood was successfully demonstrated. The diagnosis process could be completed within 50 min with the sensitivity of >98% compared with the test results generated by real-time PCR, with individual diagnoses being completed in <50 min (faster than the standard laboratory-based PCR). The tests, which enabled the diagnosis of malaria species in patients from a finger prick of whole blood, were both highly sensitive and specific, detecting malaria in 98% of infected individuals in a double-blind first-in-human study.

The paper/polymer microfluidic devices provide an easy-fabrication and fully integrated closed platform that can

effectively manipulate liquid and prevent reagent evaporation during LAMP reactions. In such hybrid systems, paper is usually employed for the simple and reliable isolation, purification, and storage of nucleic acids for diagnostic applications.¹²³ The paper substrate has also been innovatively used for storage of nucleic acid primers for LAMP reactions to improve the molecular diagnostic performance. For instance, Li and his co-workers developed a paper/PDMS hybrid microfluidic device for instrument-free diagnosis of bacterial meningitis (see Fig. 5A-a and b).^{14,15} In this hybrid microfluidic device, a paper disc (Whatman #1 chromatography paper) was placed inside each of the LAMP zones, serving as a porous 3D storage substrate for preloaded primers for interaction-based LAMP assays. It was found the paper substrate inside the hybrid microfluidic device facilitated the uniform distribution of primers for LAMP reactions (Fig. 5A-c). It is also demonstrated that the hybrid microfluidic device enabled a stable diagnostic performance for a much longer period of time than a paper-free non-hybrid system, as shown in Fig. 5A-d. The performance of LAMP assays from hybrid devices with paper inside could maintain 94% after 2 months and 85% after 3 months, while the LAMP performance from non-hybrid microfluidic devices without paper inside reduced by ~40% in the first two months. This phenomenon is mainly because that the highly interwoven paper fibers on which primers are physically adsorbed provide a 3D protection matrix for primers from harsh environmental elements without the loss in the air as aerosols. The capabilities of the paper matrix for storage and protection of nucleic acids have also been demonstrated by using paper to collect and store biological samples such as bloodstains for a long-term forensic nucleic acid analysis and pathogen detection. In addition, it is noteworthy in this work that they used a centrifuge-free lysis protocol by simply mixing the bacteria in human biological samples with a lysis buffer and incubating the mixture at room temperature for about 10 min. Then 3 μL of the lysate mixture was used for LAMP reactions without any inhibitory issues observed. This lysis approach was compatible with LAMP reactions. It also provided a simple method for direct detection of microorganisms without the requirement of either the conventional or on-chip nucleic acid extraction that involves multiple steps and buffers for cell lysis, washing, and elution. They further demonstrated broader applications of the paper/polymer microfluidic approach for detection of a whooping cough-causing bacterium, *B. pertussis*. Within 45 minutes, the LOD of 5 copies per LAMP zone for *B. pertussis* was achieved without using any specialized instruments.¹⁰⁶ High specificity and high sensitivity of the hybrid microfluidic approach were validated by testing 100 human clinical samples, which were comparable with the costly qPCR test.^{105,125}

With the integration of LAMP, another paper/PDMS/glass hybrid device was developed for multiplexed foodborne pathogen detection.¹²⁶ The device contained four layers, including a top PDMS layer for sample introduction, a

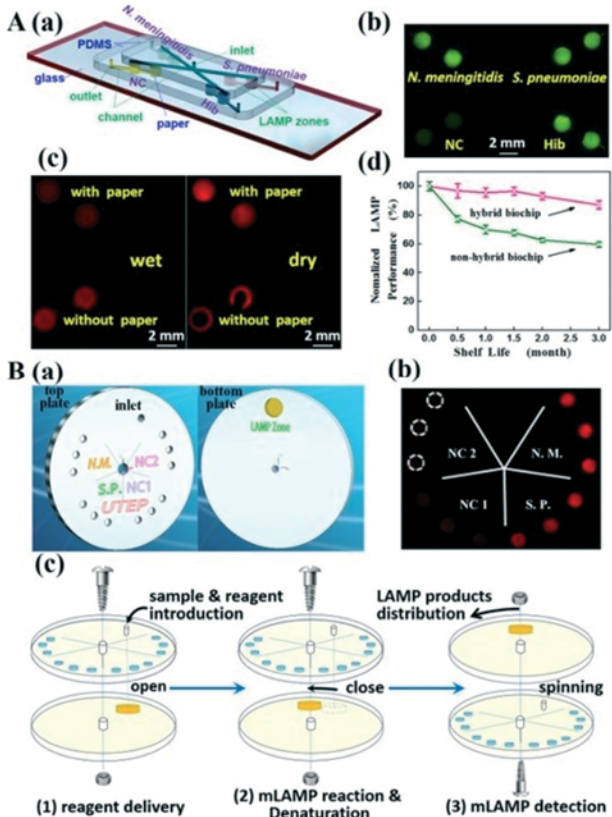


Fig. 5 Paper/polymer hybrid microfluidic devices for nucleic acid analysis. (A) A paper/PDMS hybrid microfluidic device for multiplexed and instrument-free diagnosis of bacterial meningitis. (a) Schematic of the paper/PDMS hybrid microfluidic device. (b) Direct detection of *N. meningitidis*, *S. pneumoniae*, and Hib bacteria spiked in artificial cerebrospinal fluids (ACSF); (c) fluorescence images of Cy3-labelled primers preloaded in LAMP zones with and without paper inside at wet and dry conditions. When LAMP zones became dry, primers in LAMP zones with paper could be still uniformly distributed, while primers in paper-free LAMP zones accumulated on the edge. (d) Evaluation and comparison of LAMP performance between hybrid devices with paper inside and non-hybrid devices without paper inside over a period of 3 months. Reprinted with permission from ref. 14 and 15. Copyright 2018 Elsevier and 2018 American Chemical Society. (B) A paper/PMMA hybrid microfluidic SpinChip for multiplex quantitative LAMP detection. (a) 3D schematic of the exploded view of the SpinChip. (b) The fluorescence image of nanosensor detection microzones with paper for detection of meningitis pathogenic microorganisms. (c) Working principle of the microfluidic SpinChip: one of the plates is manually spun to facilitate three different stages during the whole multiplexed LAMP detection: (1) reagent delivery, (2) mLAMP reaction and denaturation, and (3) mLAMP detection. Reprinted with permission from ref. 2. Copyright 2017 Royal Society of Chemistry.

middle PDMS layer with three reaction chambers, a chromatography paper disk as a 3D substrate for primer pre-loading, and a glass slide for structural support. Compared to the previous chip design, several changes were made in this method. An automatic sample introduction (self-priming) method was used due to the high gas solubility of PDMS. Basically, the PDMS was first degassed in vacuum, and the suction of the reagent solution was obtained uniformly in each chamber. The chip was then sealed by

injecting sealing oil, which was used to isolate each reaction chamber. Besides, a waterproof membrane was added in the top layer to decrease evaporation during LAMP. The device was applied to detect foodborne pathogens, *S. aureus* and *Vibrio parahaemolyticus*, with the LODs of 21.5 and 20.9 copies per μL , achieving around 100-fold higher sensitivity than those in conventional PCR methods.¹²⁷

DNA hybridization. Despite the growing attention of LAMP for infectious disease diagnosis, multiplexed LAMP (mLAMP) that amplifies several DNA targets in one reaction for simultaneous detection of multiple pathogens is challenging to achieve. This is mainly due to the lack of an effective detection method to identify the complicated LAMP amplicons (a mixture of different sizes of ladder-pattered stem-loop DNA sequences) from different pathogenic microorganisms. The Li group developed a paper/PMMA hybrid microfluidic SpinChip integrated with species-specific ssDNA probe-functionalized GO nanosensors and achieved simple quantitative mLAMP detection.² In this SpinChip, a single microzone in the bottom PMMA plate was designed for the mLAMP reaction where multiple DNA targets were isothermally amplified, and multiple detection microzones in the top PMMA plate were designed for identification and quantification of the amplified DNA targets based on the extraordinary distance-dependent fluorescence quenching property of GO (Fig. 5B-a and b). A paper disc (Whatman #1 chromatography paper) placed inside each of the detection microzones facilitated the integration of GO nanosensors without any complicated surface modifications and the uniform absorption of amplified DNA targets. The novel CD-like format of the SpinChip facilitated simple reagent transfer by simply rotating the PMMA plates, avoiding the use of complicated pneumatic values (Fig. 5B-c). The hybrid SpinChip was successfully demonstrated for quantitative identification of two main pathogens that cause serious bacterial meningitis, *Neisseria meningitidis* (*N. meningitidis*), and *Streptococcus pneumoniae* (*S. pneumoniae*), with high specificity. The LODs for *N. meningitidis* and *S. pneumoniae* were 6 and 12 DNA copies per assay. The whole assay process took about 1 hour, during which no washing or amplicon purification steps were needed. This Spinchip method has successfully addressed a major problem of mLAMP in identification and quantitation of multiple targets.

4.2.2 Protein analysis. In the development of paper/polymer hybrid devices for the protein analysis, lateral flow assays (LFAs) have been widely used for low-cost, qualitative, and semi-quantitative detection of different biomarkers especially in resource-limited settings as they are easy to use and inexpensive.¹²⁸ He *et al.* developed a hybrid paper/polymer chip with electro-wetting valves without external pumping equipment for sequential fluid delivery and colorimetric detection of T7 bacteriophage.¹²⁹ Nitrocellulose membrane was bound onto a polyethylene terephthalate (PET) layer with double-sided pressure-sensitive adhesive tape. They could test 10^8 PFU per mL of T7 bacteriophage with the total immunoassay time of 40 minutes. A few other

variations of LFA have been reported. For instance, Yuzon *et al.* developed a paper/plastic hybrid chip integrated with sandwich format LFA for dengue nonstructural protein 1 (NS1) antigen detection.¹³⁰ The chip consisted of a wax printed film, a baked NC membrane, and a PMMA sheet with a conjugation pad, which was assembled by using double-sided adhesive tape. Attachment of the engraved PMMA layer increased the structural support while the engraved hole in the PMMA layer allowed the integration of the conjugation pad into the system. The device was able to detect a concentration of dengue NS1 of at least 84.66 ng mL⁻¹. Paper/polymer hybrid devices have also been used for the enhancement of assay performance leveraging the advantage of both paper-based and centrifugal microfluidic platforms. Wiederoder *et al.* manipulated the fluid flow by balancing the capillary force of paper inserts with the centrifugal force generated by disc rotation to enhance the signal of a colorimetric LFA for detection of *E. coli*.¹³¹ They achieved LOD of 10⁵ colony forming units (CFUs) per mL which is a 100× improvement over a similar paper-based LFA.

Paper-based ELISA (enzyme-linked immunosorbent assay) has been extensively used for biomarker detection but has several limitations such as low performance in flow control and the need for repeated micropipetting for adding reagents and washing all the zones, limiting its application for high-throughput detection. The Li group developed a 56-microwell paper/PMMA hybrid microfluidic microplate for the rapid detection of several biomarkers of infectious disease.⁴⁰ Funnel-shaped microwells with paper inserts facilitated rapid immobilization of biomolecules and reagent delivery channels from the PMMA layer helped to transfer reagent to multiple microwells to avoid repeated manual pipetting. The LODs for multiplexed detection of immunoglobulin G (IgG) and hepatitis B surface antigen (HBsAg) were found comparable to commercial ELISA kits, but the assay could be completed using a common office scanner instead of an expensive microplate reader within an hour. Using a similar technique, Busin *et al.* fabricated another hybrid paper-based microfluidic platform (multi-pad paper plate) that was compatible with 96-well microplates.¹⁰³ Paper and lamination sheets were designed and cut in the desired format using laser micromachining and then laminated to produce the final hybrid device. A sandwich ELISA for the detection of bovine haptoglobin (Hp), a marker for inflammation in animals, was achieved with the LOD of 0.73 µg mL⁻¹. Draz and co-workers reported a paper/plastic hybrid microchip consisting of three-layer substrates: a cellulose paper substrate with screen printed electrodes assembled together with the transparent plastic sheet using double-sided adhesive.¹³² This low-cost and easy to fabricate device successfully performed multiplexed detection of different targets including liver and colon cancer protein biomarkers, with LODs for 100 ng mL⁻¹, 10³ particles per mL, and 100 copies per mL for alpha-fetoprotein (AFP) and carcinoembryonic antigen (CEA), intact Zika virus, and human papillomavirus nucleic acid amplicons, respectively.

More recently, the Li group also reported a PMMA/paper hybrid plug-and-play (PnP) reusable microfluidic device for high-sensitivity immunoassays through analyte enrichment and efficient passing-through washing.¹³³ The integration of a hybrid system significantly expanded the linear dynamic range from three orders of magnitude in a common paper-based device to a wide range of six orders of magnitude in the PnP hybrid device along with a 10-fold increase in detection sensitivity as compared to a commercial colorimetric assay.

Smartphone-based platforms have been reported in paper hybrid microfluidic devices, which can reduce the diagnostic cost and instrumentation ultimately making them more user-friendly and portable. Garg *et al.* fabricated a nitrocellulose/PDMS hybrid device that did not require external pumping for immunoassays.¹³⁴ Pumping was achieved using cavity-induced microstreaming in the microfluidic platform. The assay could be done within 18 min using an Android app. Similarly, Jalal *et al.* developed a paper/plastic hybrid device for the smartphone-based optical colorimetric analysis using an Android app.³⁹ The device was capable of colorimetric analysis of glucose, protein, pH, and red blood cell (RBC) with 40 µL of urine using a finger-actuating micro-pump. The device consisted of a paper-based reagent strip, which was embedded into the microchannel of a PC sheet. The outlet of the microchannel was connected to an elastic PDMS micropump as shown in Fig. 6A. Hybrid material combine advantages of both paper and plastic without extensive processing and modification. Finger force was applied to initiate negative pressure on the disposable PDMS micropump to move the sample solution into the device chamber. A smartphone was used to capture the image to be processed by the Android app. By integrating the strip sensor in the LOC device for urine analysis, the hybrid device improved the time-dependent inconstancy of the conventional dipstick-based urine strip, and the smartphone app used for image analysis enhanced the visual assessment of test strip. They could detect a wide range of concentrations that are in the clinical detection range for glucose (0–350 mg dL⁻¹), proteins (0–2000 mg dL⁻¹), pH (5.25–7.5), and RBC (0–280 RBC per µL).

Paper hybrid devices have also been used for stable storage of reagents for different applications. Krauss *et al.* developed a paper/polyester hybrid device for the colorimetric detection of total protein, human serum albumin (HSA), cocaine, 2,4,6-trinitrotoluene (TNT), and iron(III).¹³⁵ Long-term storage capabilities for tetrabromophenol blue, bromocresol green, cobalt thiocyanate, tetramethylammonium hydroxide, hydroxylamine, and 1,10-phenanthroline were accessed by storing these reagents in paper punches in 2.3 mm diameter chambers with a vent and inlet port. They observed no loss in color reactivity over 10 weeks. In addition, the correlation of data with different analysis methods (*i.e.*, ImageJ, image analysis on a scanner with that on a smartphone) was obtained ($R^2 = 0.985$).

4.2.3 Whole-cell detection of microorganisms. Using aptamers for the recognition of intact bacterial cells, Li and

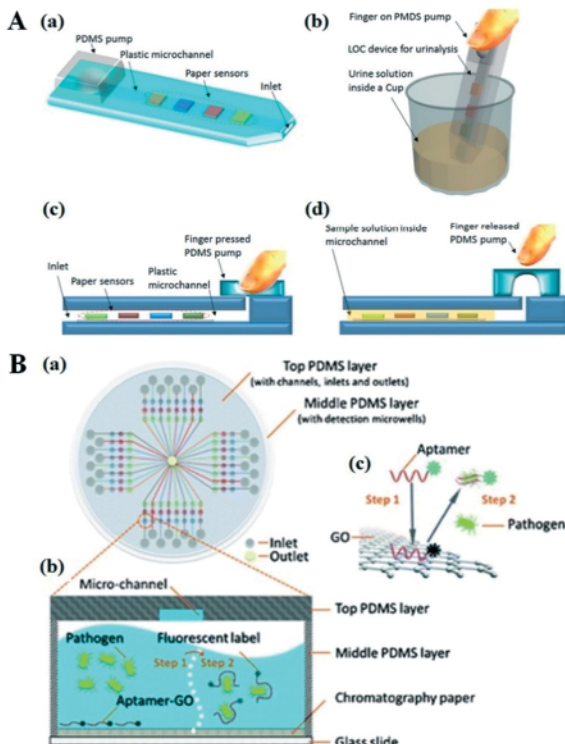


Fig. 6 Paper/polymer hybrid microfluidic devices for protein (A) and whole-cell pathogen detection (B). (A) Schematic of a hybrid microfluidic device for urinalysis. (a) The layout of the hybrid device made of patterned PC and paper. (b–d) Operational steps including a urine solution inside a cup (b), applying finger force to initiate negative pressure to move the sample solution into the device chamber (c), and the solution flows into the device chamber to react with the reagent pads (d). Reprinted with permission from ref. 39. Copyright 2018 American Chemical Society. (B) Schematic illustration of the PDMS/paper hybrid microfluidic system for one-step multiplexed detection of intact pathogenic cells. (a) Microfluidic biochip layout; (b) and (c) illustrate the principle of the one-step “turn-on” detection approach based on the interaction among GO, aptamers, and pathogens. Reprinted with permission from ref. 38. Copyright The Royal Society of Chemistry.

co-workers developed a paper/PDMS/glass hybrid microfluidic biochip for one-step multiplexed detection of intact foodborne bacterial pathogens (see Fig. 6B).³⁸ The system included a top PDMS layer for reagent delivery with inlet reservoirs and one shared waste reservoir, a bottom PDMS layer with 96 microwells for incubation and detection, a piece of chromatography paper inserted into each microwell, and a glass slide as the support. Paper was used herein serving as the substrate to adsorb the aptamer-functionalized graphene oxide (GO), which facilitated biosensor immobilization with no need for complicated surface modification. Before the assay, aptamers were adsorbed on the GO surface and the fluorescence of aptamers was quenched. In the presence of the target pathogen, aptamers were induced to liberate from GO, leaving fluorescence recovered. The one-step “turn-on” pathogen detection was approached for *Lactobacillus acidophilus* (*L. acidophilus*) and the assay took only 10 min with a ready-to-use chip. In addition, the multiplexed

pathogen detection was also investigated involving two foodborne bacterial pathogens, *S. aureus*, and *Salmonella enterica* (*S. enterica*). The LODs for two pathogens were determined to be 61.0 CFU per mL and 800 CFU per mL, respectively. The accuracy of the presented method was evaluated with the high recovery of spiked samples in the range of 92.9–107.8%. This pioneering hybrid microfluidic biochip provided a promising platform for simple and rapid detection of multiple pathogens. Thereafter, more and more paper/polymer hybrid devices have been developed.

Similarly, Xu *et al.* presented another paper/PDMS hybrid microfluidic chip for one-step identification and antimicrobial susceptibility testing (AST) for multiple uropathogens.¹³⁶ The chip contained a top PDMS layer with a sample introduction channel and holes as the inlet, outlet, and air vents, a middle PDMS layer with holes and connected channels, and a nonfeatured bottom PDMS layer. All layers were bonded together *via* plasma treatment, and paper substrates with preloaded antimicrobial agents and chromogenic medium were embedded between the middle and the bottom layer, forming the culture chambers. Each chamber was connected to the sample introducing channel as well as the air vent, which was sealed with a polyvinylidene fluoride (PVDF) membrane using double-layered adhesive tape. Three types of bacterial cells, *S. aureus*, *E. coli*, and *Enterococcus faecalis* (*E. faecalis*), were tested by using this device with the colorimetric assay, which was based on the interaction between species-specific enzymes and chromogenic substrates. Paper substrates were beneficial in the observation and interpretation of color change due to the white color as a strong contrast. The ASTs of clinical urine samples were further applied to the on-chip assay within 15 h and the results showed coincidence rates in the range of 83.3–100% in comparison with those from the conventional method. This hybrid microfluidic device enables a simple and straightforward visual measurement for multiple pathogens.

4.2.4 3D cell culture. Several paper hybrid devices for 3D cell culture involving quantification measurements have been reported using glass and PMMA as hybrid substrates. For example, a simple paper/glass hybrid platform for 3D cell culture was designed and integrated with the impedance measurement technique by Lei and the co-workers (Fig. 7).¹³⁷ In the platform, the filter paper was patterned with an array of circular microchambers by wax printing. Cancer cells (from the nasopharyngeal carcinoma (NPC)-derived cell line) were encapsulated in 1% (w/v) agarose hydrogel suspension, which was then pipetted to and permeated through the microchambers. As such, cells/hydrogel construct was generated and confined by the microchamber after gelation. The NPC Cells were cultured on the platform in a 3D model. After cell culture, paper was assembled with a glass slide integrated with ten pairs of coplanar electrodes, which were fabricated *via* Cr/Au deposition and used to measure impedance signals. The non-invasive quantification of cell proliferation up to 3 days was herein achieved by periodical

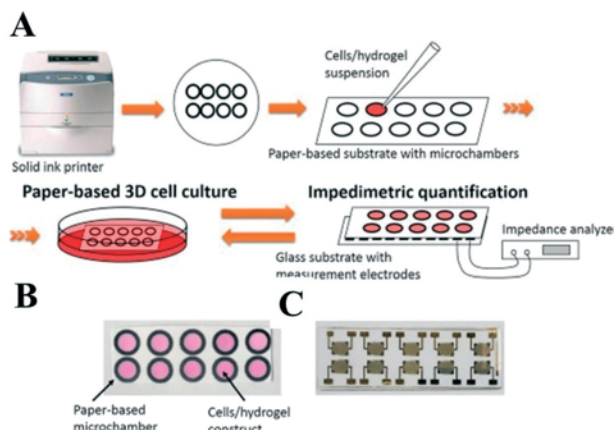


Fig. 7 Paper/polymer hybrid microfluidic devices for 3D cell culture. The procedure of the impedimentic quantification of cell proliferation using the paper/glass hybrid microchambers. (A) Illustration of cell seeding, culture, and measurement processes. (B) Photograph of the cells/hydrogel constructed in the microchambers. (C) Photograph of the glass substrate with measurement electrodes. Reprinted with permission from ref. 137. Copyright 2016 Elsevier.

impedance measurement. Another high throughput 3D cell culture and impedimentic screening of chemosensitivity of cancer cells were conducted on a similar paper/glass hybrid platform.¹³⁸ Paper substrate with microwells was used for 3D cell culture, in which cancer cells were initially encapsulated in the 0.5% (w/v) agarose hydrogel. The electrodes were fabricated on the glass from Cr/Au (200/1000 Å) by standard microfabrication including metal deposition, photolithography, and metal etching. Two human hepatoma cell lines (Huh7 and HepG2) were selected as tumorigenic cells and non-tumorigenic cells, respectively. Cell viability was studied *via* the impedance measurement at 24 and 48 h during cell culturing. The chemosensitivity was investigated *via* the high throughput impedimentic drug screening by evaluating the drug efficacy of doxorubicin and etoposide in both cell types. The paper-based device could be returned to the incubator after measurement due to the non-invasive approach. The results displayed that Huh7 cells had higher drug resistance than HepG2 cells, while doxorubicin showed higher efficacy than etoposide in the treatment of hepatocellular carcinoma.

Lei *et al.* also developed a paper/PMMA hybrid 3D cell culture microfluidic platform to study the cellular crosstalk and the related signaling pathways.¹³⁹ The filter paper substrate was patterned using wax printing, obtaining microreactors with a circular shape (10 mm in diameter) in the center and four square shapes ($5 \times 5 \text{ mm}^2$) on the neighboring sides. Prior to cell seeding, a collagen solution was added onto the paper substrate preparing for gel-free cell culture. Different types of cells (*i.e.*, Huh7, HepG2, and BM-1) were directly applied to the microreactors and anchored in the paper filters through collagen, avoid being washed away. PMMA was engraved to form diffusion channels and loaded with 0.5% (w/v) agarose hydrogel to maintain the wettability

of microreactors and provide nutrients to cells. After cell seeding, the paper substrate was placed on the PMMA plate, in which secretions from cells could diffuse through the hydrogel-infused microchannels and affect the neighboring cells. Quantification of cell proliferation was conducted using colorimetric signals *via* the water-soluble tetrazolium salt (WST-1) assay after incubation at 37 °C for 1 h. Results showed that aberrant cell proliferation of the affected cells was induced by the secretions from transfected cells. Moreover, cell phosphorylation of EGFR, cell morphology, and gene expression extracted from the cultured cells were also investigated, offering a useful platform for the investigation of the cellular crosstalk. Alternatively, a paper/PDMS/PMMA hybrid device was fabricated for 3D cell culture, cell viability screening, and protein expression studies under different chemical gradients.¹⁴⁰ A paper sheet was used to capture cells and provide a 3D cell culture environment. PDMS was used to fabricate microchannels for chemical delivery, with PMMA as a sealing layer. Chemical gradients were generated along with the paper sheet in this hybrid device due to the molecular diffusion, which was applied to study the response of Hela cervical cancer cells in a 3D culture environment. Furthermore, by adjusting the gradient of chemicals, such as nutrients, cytokines, and anti-cancer drugs (doxorubicin), the activation of the respective signal pathway was identified and studied under different stimulations.

5. Other emerging hybrid microfluidic systems

In addition to the above three main hybrid microfluidic systems, there are some innovative microfluidic devices that have been explored recently, involving materials like tape, self-adhesive laminating sheets, cotton thread, *etc.*, as summarized in Table 2.

5.1 Other paper-based emerging hybrid microfluidic systems

Paper/tape hybrid microfluidic systems. Generally, the paper/tape hybrid microfluidic devices are simply fabricated by stacking layers of paper and tape, achieving a 3D reconfigurable structure with multiple channels at different layers.¹⁴¹ Rodriguez *et al.*¹⁴² presented a foldable multiple-layer paper/tape fluidic chip that combined nucleic acid extraction, LAMP, and lateral flow detection *via* immuno-chromatographic strips. The tape in the chip served as a base material to provide a hydrophobic barrier surrounding the paper components and prevent evaporation during LAMP reactions. This chip also included several other components: a polyethersulfone (PES) filter paper-based sample port used for the introduction of samples and reagents and the capture of nucleic acids for LAMP reactions; a cellulose blotting paper disk as an absorbent pad for lysing and washing waste; detection test strips consisting of streptavidin-conjugated gold nanoparticles for immuno-chromatographic assays. This

fully integrated system was demonstrated by detecting human papillomavirus (HPV) DNA directly from patient cervical specimens in less than 1 hour for rapid and early diagnosis of cervical cancer.

Paper/glass microcapillary hybrid microfluidic systems. A fully integrated FTA paper/glass microcapillary hybrid microfluidic device was reported for sample-to-answer molecular diagnosis.¹⁴³ In this hybrid microfluidic system, the FTA paper was used for nucleic acid capture and purification. Different segments of reagents including lysis buffer, washing buffer, and LAMP reaction mix were preloaded in the microcapillary in sequence. After loading samples, the FTA paper-based DNA extraction and LAMP reaction were performed by loading the corresponding reagents. The whole procedure could be completed within 150 min. This paper/microcapillary hybrid microfluidic system required minimal user operation, simply using a displacement pipet tip and a hand-held UV-flashlight for endpoint fluorescence-based detection without relying on any bulky instruments. The system was successfully demonstrated by a screening assay of single nucleotide polymorphisms (SNPs) typing of the CYP2C19 gene from 200 nL of freshly drawn finger blood samples.

5.2 Thread-based hybrid microfluidic systems

Except for the widely used substrate materials (*e.g.*, polymer and paper), new substrates such as cotton threads with the wicking property and flexibility, have also been demonstrated to be suitable for the fabrication and application of low-cost microfluidic platforms.¹⁴⁴ The thread has 3D passageways in sewed materials, which can transport liquid *via* the capillary wicking without the need for a barrier. In addition, liquids can penetrate from the thread into other hydrophilic porous materials. Therefore, the thread can be integrated with paper to form a hybrid microfluidic platform with enhanced sample delivering efficiency for qualitative or semi-quantitative analysis.

Lin *et al.*¹⁴⁴ developed a novel paper/cotton hybrid microfluidic platform for *in vitro* diagnostics, which used cotton as a flow channel and chromatography paper as a reaction zone for semi-quantitative analysis. The color intensity was distinguishable by the naked eye or analysed using the software ImageJ for statistical/semi-quantitative analysis. By using artificial samples, clinically relevant ranges of approximately 0.38–30 mM for urine protein, 0.156–2.5 mM for nitrite, 7.8–125 mM for urobilinogen, and 100–1600 mM for uric acid were analyzed. Jia *et al.* developed an immune-chromatographic assay for carcinoembryonic antigen (CEA) detection on a cotton thread/paper hybrid device using carbon nanotube/gold nanoparticles (CNT/GNPs) nanocomposite reporter probes.¹⁴⁵ As shown in Fig. 8A, the acid-treated CNT was functionalized with PDDA (poly(diallyldimethylammonium chloride), as a bridge), GNPs, and then detection antibodies to form the probes. The whole device consisted of a sample pad, a cotton thread, and an

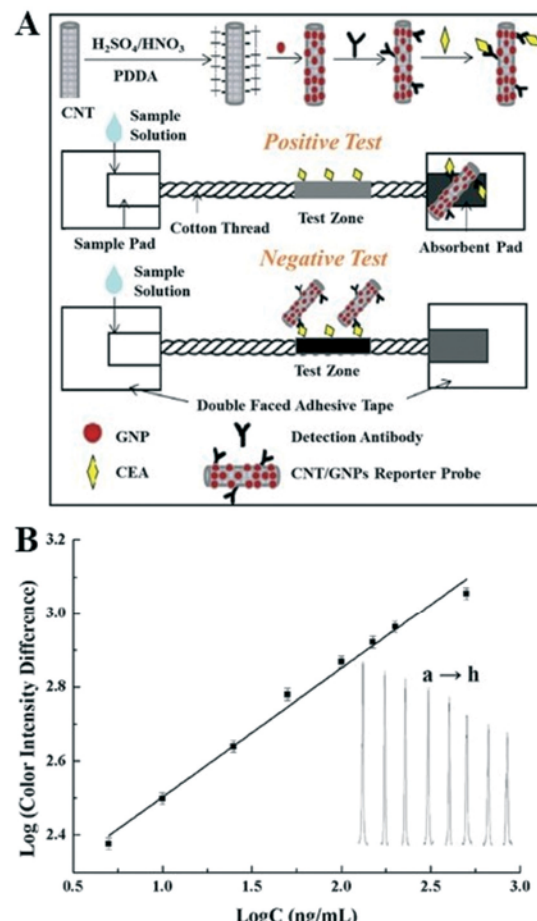


Fig. 8 Other emerging paper-like hybrid microfluidic devices for cost-effective diagnostics. (A) Principle of using a cotton thread/paper hybrid device based on CNT/GNPs nanocomposite reporter probes for CEA detection. (B) Quantitative analysis of CEA in human serum samples using the cotton thread/paper hybrid device. Sample a to h: 5, 10, 25, 50, 100, 150, 200, and 500 ng mL⁻¹. Reprinted with permission from ref. 145. Copyright 2017 Elsevier.

absorbed pad. CEA was dispensed onto the cotton thread to form a test zone. A filter paper strip as the absorbent pad was attached at the downstream end of the thread, and glass fiber as the sample pad was covered on the other end of thread onto a clean plastic pad using double-sided tape. When running the assay, CEA with different concentrations was incubated with the CNT/GNPs nanocomposite reporter probes to form sample solutions, which were simply loaded onto the sample pad. Quantitative analysis of the optical intensity of color bands on the test zone was performed (Fig. 8B). The cotton thread-based biosensor had the LOD of 2.32 ng mL⁻¹ for CEA in human serum samples, increasing the sensitivity by four magnitudes compared to the conventional CNT-based lateral flow assay. Likewise, using gold nanoparticle trimer reporters on a similar device, the lung cancer-related biomarker, human ferritin antigen was detected with the LOD of 10 ng mL⁻¹.¹⁴⁶

Alternatively, Nilghaz *et al.* developed a thread-based microfluidic device for rapid semi-quantitative analysis of

analytes (e.g., BSA and nitrite) by measuring the length of color change on indicator-treated threads.¹⁴⁷ The device was fabricated using two types of threads, cotton and polyester, for capillary wicking of liquid samples. The cotton and polyester threads were treated with different colorimetric indicator reagents corresponding to different analytes. When performing the test, the deposited reagents (e.g., tetrabromophenol blue (BPB) and Griess reagent) reacted with the corresponding analytes (e.g., BSA and nitrite) in samples and generated colored zones with different lengths on the threads that correlated with the concentrations of analytes. This approach was successfully demonstrated by performing colorimetric assays for two clinical biomarkers, BSA and nitrite, in simulated human urine samples. The semi-quantitative analysis was achieved by measuring the length of generated color zones on the threads corresponding to the analytes. The linear ranges for detecting BSA and nitrite were 0–1.5 mg mL⁻¹ and 0–1000 µM, respectively.

6. Conclusions and perspectives

This article reviews the recent development of different types of low-cost hybrid microfluidic systems based on PDMS, thermoplastics, paper, and some other emerging substrates. In this review, we introduce and discuss the broad biomedical applications of these polymer and paper hybrid microfluidic systems including nucleic acid analysis, protein analysis, whole-cell detection, 3D cell culture, organ-on-a-chip, and tissue engineering, as summarized in Tables 1 and 2. The polymer- and paper-based hybrid microfluidic devices are promising and superior platforms with key features of biocompatibility, ease of fabrication, high integration profile, and low cost. As such, these low-cost and portable hybrid devices have great potential for POC detection of various diseases such as the recent widely-spread COVID-19 caused by SARS-CoV-2,¹⁴⁸ especially in low-resource settings such as rural areas and developing nations. More importantly, by combining different substrates with their own and supplemental advantages with each other, the hybrid microfluidic systems generate unprecedented characteristics that benefit the biomedical research and applications.

Despite these benefits, polymer and paper hybrid microfluidic systems are still in the early stage of development. There are some limitations to be addressed in order to achieve broader applications of hybrid microfluidic devices. For example, most hybrid devices have been fabricated *via* simple assembly from two or more single substrate-based microfluidic compartments, while the fabrication techniques of a whole set of hybrid microfluidic devices are rather limited. In addition, the resolution of hybrid devices (such as paper/polymer hybrid devices) is limited by current microfabrication methods, which is in need of improvement by addressing technological challenges and implementing new technology such as 3D printing.

With the improvement of microfluidic techniques, the polymer and paper hybrid microfluidic systems are anticipated to be employed in wider applications from low-cost diagnostics to controlled drug delivery and chemical synthesis. In addition, more novel hybrid microfluidic systems are expected to be developed with the emergence of various new engineered materials in the near future (e.g., stimulus-responsive hydrogels).^{22,48,149} Moreover, we envision that different types of hybrid microfluidic devices can be integrated into a total micro-bioanalysis system that can perform complicated processing and provide comprehensive information, such as a serial of studies of stem cells or circulating tumor cells (CTCs) from the single cell separation and isolation to the evaluation of drug treatment.^{4,150,151} Nanomaterial-functionalized biosensors such as metal-organic frameworks (MOFs)-functionalized aptasensors,^{104,152–157} smartphone-based detectors,¹⁵⁸ and thermometer-based quantitative photothermometric biosensing^{17,154,155,159} will also cause more attention, and become more widely incorporated in hybrid microfluidic devices. At last, more and more applications from these unique hybrid platforms would gradually set off the commercialization of hybrid microfluidic devices, and the successful translation from a laboratory to the market will lead to greater impacts on our economy, healthcare, and society.

Conflicts of interest

There are no conflicts to declare.

Acknowledgements

We would like to acknowledge the financial support from the National Institute of Allergy and Infectious Disease of the NIH (R21AI107415), the U.S. NSF (IIP2122712, IIP2052347, IIP1953841, and DMR1827745), DOT (CARTEEH), the University of Texas at El Paso (UTEP) for the IDR Program, the Philadelphia Foundation, and the Medical Center of the Americas Foundation. Prior financial support from the National Institute of General Medical Sciences of the NIH (SC2GM105584), the NIH RCMI Pilot Grant, NSF, the University of Texas (UT) System for the STARS award, the NIH BUILDing Scholar Summer Sabbatical Award, and the Multidisciplinary Research Award Program (MRAP) and the URI Program from UTEP is also gratefully acknowledged.

References

- 1 X. F. Wei, W. Zhou, S. T. Sanjay, J. Zhang, Q. J. Jin, F. Xu, D. C. Dominguez and X. J. Li, *Anal. Chem.*, 2018, 90, 9888–9896.
- 2 M. W. Dou, S. T. Sanjay, D. C. Dominguez, S. H. Zhan and X. J. Li, *Chem. Commun.*, 2017, 53, 10886–10889.
- 3 M. Dou, S. T. Sanjay, M. Benhabib, F. Xu and X. Li, *Talanta*, 2015, 145, 43–54.
- 4 H. Tavakoli, W. Zhou, L. Ma, S. Perez, A. Ibarra, F. Xu, S. Zhan and X. Li, *TrAC, Trends Anal. Chem.*, 2019, 117, 13–26.

5 M. W. Dou, J. Lopez, M. Rios, O. Garcia, C. Xiao, M. Eastman and X. J. Li, *Analyst*, 2016, 141, 3898–3903.

6 S. T. Sanjay, M. W. Dou, G. L. Fu, F. Xu and X. J. Li, *Curr. Pharm. Biotechnol.*, 2016, 17, 772–787.

7 M. W. Dou, J. M. Garcia, S. H. Zhan and X. J. Li, *Chem. Commun.*, 2016, 52, 3470–3473.

8 H. Jayamohan, V. Romanov, H. Li, J. Son, R. Samuel, J. Nelson and B. K. Gale, *Molecular Diagnostics*, 3rd edn, 2017, pp. 197–217.

9 S. T. Sanjay, G. Fu, M. Dou, F. Xu, R. Liu, H. Qi and X. Li, *Analyst*, 2015, 140, 7062–7081.

10 S. T. Sanjay, W. Zhou, M. W. Dou, H. Tavakoli, L. Ma, F. Xu and X. J. Li, *Adv. Drug Delivery Rev.*, 2018, 128, 3–28.

11 F. Shen, Y. Li, Z. Liu and X. Li, *Microfluid. Nanofluid.*, 2017, 21, 66.

12 F. Shen, X. Li and P. C. H. Li, *Biomicrofluidics*, 2014, 8, 014109.

13 X. J. Li and Y. Zhou, *Microfluidic Devices for Biomedical Applications*, Woodhead Publishing, 2013.

14 M. Dou, S. T. Sanjay, D. C. Dominguez, P. Liu, F. Xu and X. Li, *Biosens. Bioelectron.*, 2017, 87, 865–873.

15 M. W. Dou, D. C. Dominguez, X. J. Li, J. Sanchez and G. Scott, *Anal. Chem.*, 2014, 86, 7978–7986.

16 Q. Jin, L. Ma, W. Zhou, Y. Shen, O. Fernandez-Delgado and X. J. Li, *Chem. Sci.*, 2020, 11, 2915–2925.

17 G. Fu, Y. Zhu, K. Xu, W. Wang, R. Hou and X. Li, *Anal. Chem.*, 2019, 91, 13290–13296.

18 A. Gonzalez, L. Estala, M. Gaines and F. A. Gomez, *Electrophoresis*, 2016, 37, 1685–1690.

19 D. Agustini, M. F. Bergamini and L. H. Marcolino, *Lab Chip*, 2016, 16, 345–352.

20 K. S. Prasad, Y. Abugalyon, C. Li, F. Xu and X. Li, *Analyst*, 2020, 145, 5113–5117.

21 W. Zhou, M. Feng, A. Valadez and X. Li, *Anal. Chem.*, 2020, 92, 7045–7053.

22 G. Fu, W. Zhou and X. Li, *Lab Chip*, 2020, 20, 2218–2227.

23 Y. Xu, X. Hu, S. Kundu, A. Nag, N. Afsarimanesh, S. Sapra, S. C. Mukhopadhyay and T. Han, *Sensors*, 2019, 19, 2908.

24 Z. Liao, Y. Zhang, Y. Li, Y. Miao, S. Gao, F. Lin, Y. Deng and L. Geng, *Biosens. Bioelectron.*, 2019, 126, 697–706.

25 F. Costantini, R. M. Tiggelaar, R. Salvio, M. Nardecchia, S. Schlaутmann, C. Manetti, H. J. G. E. Gardeniers, G. de Cesare, D. Caputo and A. Nascetti, *Biosensors*, 2017, 7, 58.

26 L. C. Lasave, S. M. Borisov, J. Ehgartner and T. Mayr, *RSC Adv.*, 2015, 5, 70808–70816.

27 T. Mayer, A. N. Marianov and D. W. Inglis, *Mater. Res. Express*, 2018, 5, 085201.

28 S. Agaoglu, M. C. Robles, C. D. Smith, S. R. Quake and I. E. Araci, *Microfluid. Nanofluid.*, 2017, 21, 117.

29 M. Tonin, N. Descharmes and R. Houdre, *Lab Chip*, 2016, 16, 465–470.

30 M. Humayun, C. W. Chow and E. W. K. Young, *Lab Chip*, 2018, 18, 1298–1309.

31 S. Wouters, J. De Vos, J. L. Dores-Sousa, B. Wouters, G. Desmet and S. Eeltink, *J. Chromatogr. A*, 2017, 1523, 224–233.

32 T. H. Yang, Y. Su and S. J. Li, *Proceedings of 2015 International Conference on Fluid Power and Mechatronics*, 2015, pp. 706–710.

33 H. Tavakoli, W. Zhou, L. Ma, Q. Guo and X. Li, *Nanotechnol. Microfluid.*, 2020, 177–209.

34 D. M. Cate, J. A. Adkins, J. Mettakoonpitak and C. S. Henry, *Anal. Chem.*, 2015, 87, 19–41.

35 J. Hu, S. Wang, L. Wang, F. Li, B. Pingguan-Murphy, T. J. Lu and F. Xu, *Biosens. Bioelectron.*, 2014, 54, 585–597.

36 M. Sher, R. Zhuang, U. Demirci and W. Asghar, *Expert Rev. Mol. Diagn.*, 2017, 17, 351–366.

37 H. Chen, Z. Li, L. Z. Zhang, P. Sawaya, J. B. Shi and P. Wang, *Angew. Chem., Int. Ed.*, 2019, 58, 13922–13928.

38 P. Zuo, X. Li, D. C. Dominguez and B. C. Ye, *Lab Chip*, 2013, 13, 3921–3928.

39 U. M. Jalal, G. J. Jin and J. S. Shim, *Anal. Chem.*, 2017, 89, 13160–13166.

40 S. T. Sanjay, M. W. Dou, J. J. Sun and X. J. Li, *Sci. Rep.*, 2016, 6, 30474.

41 S. T. Sanjay, M. Li, W. Zhou, X. Li and X. Li, *Microsyst. Nanoeng.*, 2020, 6, 28.

42 F. M. Pereira, I. Bernacka-Wojcik, R. S. R. Ribeiro, M. T. Lobato, E. Fortunato, R. Martins, R. Igreja, P. A. S. Jorge, H. Aguas and A. M. G. Oliva, *Micromachines*, 2016, 7, 181.

43 T. Santaniello, Y. S. Yan, A. Tocchio, F. Martello, P. Milani and C. Lenardi, *Microfluid. Nanofluid.*, 2015, 19, 31–41.

44 S. Hao, L. Ha, G. Cheng, Y. Wan, Y. Xia, D. M. Sosnoski, A. M. Mastro and S. Y. Zheng, *Small*, 2018, 14, e1702787.

45 Q. Chen, D. Wang, G. Z. Cai, Y. H. Xiong, Y. T. Li, M. H. Wang, H. L. Huo and J. H. Lin, *Biosens. Bioelectron.*, 2016, 86, 770–776.

46 M. J. Delince, J. B. Bureau, A. T. Lopez-Jimenez, P. Cosson, T. Soldati and J. D. McKinney, *Lab Chip*, 2016, 16, 3276–3285.

47 J. W. Wu, R. D. Wang, H. X. Yu, G. J. Li, K. X. Xu, N. C. Tien, R. C. Roberts and D. C. Li, *Lab Chip*, 2015, 15, 690–695.

48 M. You, Z. Li, S. Feng, B. Gao, C. Yao, J. Hu and F. Xu, *Trends Biotechnol.*, 2020, 38, 637–649.

49 M. You, L. Cao and F. Xu, *Trends Biochem. Sci.*, 2020, 45, 174–175.

50 P. Liu, X. Li, S. A. Greenspoon, J. R. Scherer and R. A. Mathies, *Lab Chip*, 2011, 11, 1041–1048.

51 E. A. Oblath, W. H. Henley, J. P. Alarie and J. M. Ramsey, *Lab Chip*, 2013, 13, 1325–1332.

52 X. Jiang, N. Shao, W. Jing, S. Tao, S. Liu and G. Sui, *Talanta*, 2014, 122, 246–250.

53 C. M. Han, E. Katilius and J. G. Santiago, *Lab Chip*, 2014, 14, 2958–2967.

54 W. Zhou, G. Fu and X. Li, *Anal. Chem.*, 2021, 93, 7754–7762.

55 P. Jolly, P. Damborsky, N. Madabooisi, R. R. G. Soares, V. Chu, J. P. Conde, J. Katrlik and P. Estrela, *Biosens. Bioelectron.*, 2016, 79, 313–319.

56 X. H. Liu, H. Li, Y. J. Zhao, X. D. Yu and D. K. Xu, *Talanta*, 2018, 188, 417–422.

57 J. K. Liu, J. Q. Zhao, P. Petrochenko, J. W. Zheng and I. Hewlett, *Biosens. Bioelectron.*, 2016, 86, 150–155.

58 M. Sharafeldin, G. W. Bishop, S. Bhakta, A. El-Sawy, S. L. Suib and J. F. Rusling, *Biosens. Bioelectron.*, 2017, 91, 359–366.

59 A. H. Nguyen, J. Lee, H. I. Choi, H. S. Kwak and S. J. Sim, *Biosens. Bioelectron.*, 2015, 70, 358–365.

60 Y. H. Lin and P. Y. Peng, *Anal. Chim. Acta*, 2015, 869, 34–42.

61 M. Regiart, M. A. Fernandez-Baldo, J. Villarroel-Rocha, G. A. Messina, F. A. Bertolino, K. Sapag, A. T. Timperman and J. Raba, *Anal. Chim. Acta*, 2017, 963, 83–92.

62 Y. Cao, B. Zhang, Z. Zhu, X. Xin, H. Wu and B. Chen, *Front. Bioeng. Biotechnol.*, 2021, 9, 622108.

63 J. Bae, J.-W. Lim and T. Kim, *Sens. Actuators, B*, 2018, 264, 372–381.

64 X. K. Hao, P. Y. Yeh, Y. B. Qin, Y. Q. Jiang, Z. Y. Qiu, S. Y. Li, T. Le and X. D. Cao, *Anal. Chim. Acta*, 2019, 1056, 96–107.

65 J. X. Yin, Z. Y. Zou, Z. M. Hu, S. Zhang, F. P. Zhang, B. Wang, S. W. Lv and Y. Mu, *Lab Chip*, 2020, 20, 979–986.

66 Q. Zhu, M. Hamilton, B. Vasquez and M. He, *Lab Chip*, 2019, 19, 2362–2372.

67 M. Mao, J. He, Y. Lu, X. Li, T. Li, W. Zhou and D. Li, *Biofabrication*, 2018, 10, 025008.

68 Y. Yajima, C. N. Lee, M. Yamada, R. Utoh and M. Seki, *J. Biosci. Bioeng.*, 2018, 126, 111–118.

69 H. Moghadas, M. S. Saidi, N. Kashaninejad and N. T. Nguyen, *Biomicrofluidics*, 2018, 12, 024117.

70 S. Sharghi-Namini, E. Tan, L. L. Ong, R. Ge and H. H. Asada, *Sci. Rep.*, 2014, 4, 4031.

71 E. Tan, H. H. Asada and R. Ge, *Angiogenesis*, 2018, 21, 571–580.

72 A. S. Johnson, B. T. Mehl and R. S. Martin, *Anal. Methods*, 2015, 7, 884–893.

73 V. Palacio-Castaneda, L. Kooijman, B. Venzac, W. P. R. Verdurmen and S. Le Gac, *Micromachines*, 2020, 11, 382.

74 Z. Wu, Y. Zheng, L. Lin, S. Mao, Z. Li and J. M. Lin, *Angew. Chem.*, 2020, 132, 2245–2249.

75 Q. Chen, S. Utech, D. Chen, R. Prodanovic, J.-M. Lin and D. A. Weitz, *Lab Chip*, 2016, 16, 1346–1349.

76 J. Wu, Q. Chen, W. Liu, Z. He and J.-M. Lin, *TrAC, Trends Anal. Chem.*, 2017, 87, 19–31.

77 J. H. Lee, S. K. Kim, L. A. Khawar, S. Y. Jeong, S. Chung and H. J. Kuh, *J. Exp. Clin. Cancer Res.*, 2018, 37, 1–12.

78 B. T. Mehl and R. S. Martin, *Anal. Methods*, 2019, 11, 1064–1072.

79 N. Bhattacharjee, C. Parra-Cabrera, Y. T. Kim, A. P. Kuo and A. Folch, *Adv. Mater.*, 2018, 30, e1800001.

80 L. J. Y. Ong, A. Islam, R. DasGupta, N. G. Iyer, H. L. Leo and Y. C. Toh, *Biofabrication*, 2017, 9, 045005.

81 D. Caballero, S. Kaushik, V. M. Correlo, J. M. Oliveira, R. L. Reis and S. C. Kundu, *Biomaterials*, 2017, 149, 98–115.

82 C. Tian, Q. Tu, W. Liu and J. Wang, *TrAC, Trends Anal. Chem.*, 2019, 117, 146–156.

83 L. Bakhchova, L. Jonušauskas, D. Andrijec, M. Kurachkina, T. Baravykas, A. Eremin and U. Steinmann, *Materials*, 2020, 13, 3076.

84 A. Choe, S. K. Ha, I. Choi, N. Choi and J. H. Sung, *Biomed. Microdevices*, 2017, 19, 4.

85 D. W. Lee, S. K. Ha, I. Choi and J. H. Sung, *Biomed. Microdevices*, 2017, 19, 100.

86 S. Y. Lee and J. H. Sung, *Biotechnol. Bioeng.*, 2018, 115, 2817–2827.

87 M. W. van der Helm, M. Odijk, J. P. Frimat, A. D. van der Meer, J. C. T. Eijkel, A. van den Berg and L. I. Segerink, *J. Visualized Exp.*, 2017, e56334.

88 K. Kadimisetty, S. Malla, N. P. Sardesai, A. A. Joshi, R. C. Faria, N. H. Lee and J. F. Rusling, *Anal. Chem.*, 2015, 87, 4472–4478.

89 A. M. Ortega-Prieto, J. K. Skelton, S. N. Wai, E. Large, M. Lussignol, G. Vizcay-Barrena, D. Hughes, R. A. Fleck, M. M. Thursz, M. T. Catanese and M. Dorner, *Nat. Commun.*, 2018, 9, 1–15.

90 N. P. Mortensen, K. A. Mercier, S. McRitchie, T. B. Cavallo, W. Pathmasiri, D. Stewart and S. J. Sumner, *Biomed. Microdevices*, 2016, 18, 51.

91 L. Malic, X. Zhang, D. Brassard, L. Clime, J. Daoud, C. Luebbert, V. Barrere, A. Boutin, S. Bidawid, J. Farber, N. Corneau and T. Veres, *Lab Chip*, 2015, 15, 3994–4007.

92 P. Maffert, S. Reverchon, W. Nasser, C. Rozand and H. Abaibou, *Eur. J. Clin. Microbiol. Infect. Dis.*, 2017, 36, 1717–1731.

93 S. T. Sanjay, M. Dou, J. Sun and X. Li, *Sci. Rep.*, 2016, 6, 30474.

94 C. V. Uliana, C. R. Peverari, A. S. Afonso, M. R. Cominetti and R. C. Faria, *Biosens. Bioelectron.*, 2018, 99, 156–162.

95 H. Shafiee, M. K. Kanakasabapathy, F. Juillard, M. Keser, M. Sadasivam, M. Yuksekaya, E. Hanhauser, T. J. Henrich, D. R. Kuritzkes, K. M. Kaye and U. Demirci, *Sci. Rep.*, 2015, 5, 9919.

96 J. Kim, K. Hong, H. Kim, J. Seo, J. Jeong, P. K. Bae, Y. B. Shin, J. H. Lee, H. J. Oh and S. Chung, *Sens. Actuators, B*, 2020, 316, 128094.

97 K. İçöz, Ü. Akar and E. Ünal, *Biomed. Microdevices*, 2020, 22, 48.

98 C. Chen, A. D. Townsend, E. A. Hayter, H. M. Birk, S. A. Sell and R. S. Martin, *Anal. Bioanal. Chem.*, 2018, 410, 3025–3035.

99 A. S. Munshi, C. P. Chen, A. D. Townsend and R. S. Martin, *Anal. Methods*, 2018, 10, 3364–3374.

100 J. Jeong, Y. Lee, Y. Yoo and M. K. Lee, *Colloids Surf., B*, 2018, 162, 306–315.

101 A. Ozaki, Y. Arisaka and N. Takeda, *Biofabrication*, 2016, 8, 035010.

102 U. M. Jalal, G. J. Jin and J. S. Shim, *Anal. Chem.*, 2017, 89, 13160–13166.

103 V. Busin, S. Burgess and W. M. Shu, *Sens. Actuators, B*, 2018, 273, 536–542.

104 W. Zhou, J. Sun and X. Li, *Anal. Chem.*, 2020, 92, 14830–14837.

105 M. Dou, N. Macias, F. Shen, J. Dien Bard, D. C. Domínguez and X. Li, *EClinicalMedicine*, 2019, 8, 72–77.

106 M. Dou, J. Sanchez, H. Tavakoli, J. E. Gonzalez, J. Sun, J. D. Bard and X. Li, *Anal. Chim. Acta*, 2019, 1065, 71–78.

107 G. Fu, X. Li, W. Wang and R. Hou, *Biosens. Bioelectron.*, 2020, **170**, 112646.

108 L. Ma, Y. Abugalyon and X. Li, *Anal. Bioanal. Chem.*, 2021, **413**, DOI: 10.1007/s00216-00021-03359-00218, in press.

109 H. Tavakoli, W. Zhou, L. Ma, Q. Guo and X. Li, in *Nanotechnology and Microfluidics*, Wiley, 2020, pp. 177–209.

110 Y. Xia, J. Si and Z. Li, *Biosens. Bioelectron.*, 2016, **77**, 774–789.

111 T. Akyazi, L. Basabe-Desmonts and F. Benito-Lopez, *Anal. Chim. Acta*, 2018, **1001**, 1–17.

112 K. Yamada, T. G. Henares, K. Suzuki and D. Citterio, *Angew. Chem., Int. Ed.*, 2015, **54**, 5294–5310.

113 P. Lisowski and P. K. Zarzycki, *Chromatographia*, 2013, **76**, 1201–1214.

114 L. Yu and Z. Z. Shi, *Lab Chip*, 2015, **15**, 1642–1645.

115 Y. L. Han, W. Wang, J. Hu, G. Huang, S. Wang, W. G. Lee, T. J. Lu and F. Xu, *Lab Chip*, 2013, **13**, 4745–4749.

116 R. Tang, H. Yang, J. R. Choi, Y. Gong, J. Hu, T. Wen, X. Li, B. Xu, Q. Mei and F. Xu, *Microchim. Acta*, 2017, **184**, 2141–2150.

117 W. Gan, B. Zhuang, P. Zhang, J. Han, C.-X. Li and P. Liu, *Lab Chip*, 2014, **14**, 3719–3728.

118 B. Zhuang, W. Gan, S. Wang, J. Han, G. Xiang, C.-X. Li, J. Sun and P. Liu, *Anal. Chem.*, 2015, **87**, 1202–1209.

119 W. Gan, Y. Gu, J. Han, C.-x. Li, J. Sun and P. Liu, *Anal. Chem.*, 2017, **89**, 3568–3575.

120 T. Notomi, Y. Mori, N. Tomita and H. Kanda, *J. Microbiol.*, 2015, **53**, 1–5.

121 R. Nakano, A. Nakano, Y. Ishii, T. Ubagai, T. Kikuchi-Ueda, H. Kikuchi, S. Tansho-Nagakawa, G. Kamoshida, X. Mu and Y. Ono, *J. Infect. Chemother.*, 2015, **21**, 202–206.

122 C. Liu, M. Mauk, R. Gross, F. D. Bushman, P. H. Edelstein, R. G. Collman and H. H. Bau, *Anal. Chem.*, 2013, **85**, 10463–10470.

123 C. Liu, M. G. Mauk, R. Hart, M. Bonizzoni, G. Yan and H. H. Bau, *PLoS One*, 2012, **7**, e42222.

124 J. Reboud, G. Xu, A. Garrett, M. Adriko, Z. Yang, E. M. Tukahebwa, C. Rowell and J. M. Cooper, *Proc. Natl. Acad. Sci. U. S. A.*, 2019, **116**, 4834–4842.

125 M. Dou, N. Macias, F. Shen, J. D. Bard, D. C. Domínguez and X. Li, *EClinicalMedicine*, 2019, **8**, 72–77.

126 B. Pang, K. Y. Fu, Y. S. Liu, X. Ding, J. M. Hu, W. S. Wu, K. Xu, X. L. Song, J. Wang, Y. Mu, C. Zhao and J. Li, *Anal. Chim. Acta*, 2018, **1040**, 81–89.

127 K. Chandrashekhar, S. Isloor, B. Veeresh, R. Hegde, D. Rathnamma, S. Murag, B. Veeregowda, H. Upendra and N. R. Hegde, *Folia Microbiol.*, 2015, **60**, 465–472.

128 M. S. Wiederoder, S. Smith, P. Madzivhandila, D. Mager, K. Moodley, D. L. DeVoe and K. J. Land, *Biomicrofluidics*, 2017, **11**, 054101.

129 F. He, J. Grimes, S. D. Alcaine and S. R. Nugen, *Analyst*, 2014, **139**, 3002–3008.

130 K. Yuzon, J. H. Kim and S. Kim, *BioChip J.*, 2019, **13**, 277–287.

131 M. Wiederoder, S. Smith, P. Madzivhandila, D. Mager, K. Moodley, D. L. DeVoe and K. J. Land, *Biomicrofluidics*, 2017, **11**, 054101.

132 M. S. Draz, M. Moazeni, M. Venkataramani, H. Lakshminarayanan, E. Saygili, N. K. Lakshminaraasimulu, K. M. Kochehbyoki, M. K. Kanakasabapathy, S. Shabahang, A. Vasan, M. A. Bijarchi, A. Memic and H. Shafiee, *Adv. Funct. Mater.*, 2018, **28**, 1707161.

133 S. T. Sanjay, M. H. Li, W. Zhou, X. C. Li and X. J. Li, *Microsyst. Nanoeng.*, 2020, **6**, 1–11.

134 N. Garg, D. Vallejo, D. Boyle, I. Nanayakkara, A. Teng, J. Pablo, X. Liang, D. Camerini, A. P. Lee and P. Felgner, *Procedia Eng.*, 2016, **159**, 53–57.

135 S. T. Krauss, V. C. Holt and J. P. Landers, *Sens. Actuators, B*, 2017, **246**, 740–747.

136 B. Xu, Y. Du, J. Lin, M. Qi, B. Shu, X. Wen, G. Liang, B. Chen and D. Liu, *Anal. Chem.*, 2016, **88**, 11593–11600.

137 K. F. Lei, C. H. Huang and N. M. Tsang, *Talanta*, 2016, **147**, 628–633.

138 K. F. Lei, T. K. Liu and N. M. Tsang, *Biosens. Bioelectron.*, 2018, **100**, 355–360.

139 K. F. Lei, C. H. Chang and M. J. Chen, *ACS Appl. Mater. Interfaces*, 2017, **9**, 13092–13101.

140 K. F. Lei, A. Goh and C. H. Huang, *Talanta*, 2019, **205**, 120124.

141 B. M. Jayawardane, I. D. McKelvie and S. D. Kolev, *Anal. Chem.*, 2015, **87**, 4621–4626.

142 N. M. Rodriguez, W. S. Wong, L. Liu, R. Dewar and C. M. Klapperich, *Lab Chip*, 2016, **16**, 753–763.

143 L. Zhang, Y. Zhang, C. Wang, Q. Feng, F. Fan, G. Zhang, X. Kang, X. Qin, J. Sun, Y. Li and X. Jiang, *Anal. Chem.*, 2014, **86**, 10461–10466.

144 S.-C. Lin, M.-Y. Hsu, C.-M. Kuan, H.-K. Wang, C.-L. Chang, F.-G. Tseng and C.-M. Cheng, *Sci. Rep.*, 2014, **4**, 1–12.

145 X. B. Jia, T. T. Song, Y. Liu, L. L. Meng and X. Mao, *Anal. Chim. Acta*, 2017, **969**, 57–62.

146 X. Mao, T. E. Du, L. L. Meng and T. T. Song, *Anal. Chim. Acta*, 2015, **889**, 172–178.

147 A. Nilghaz, D. R. Ballerini, X. Y. Fang and W. Shen, *Sens. Actuators, B*, 2014, **191**, 586–594.

148 X. Li and C. Yang, *Anal. Bioanal. Chem.*, 2021, **413**, DOI: 10.1007/s00216-021-03441-1.

149 Q. Shi, H. Liu, D. Tang, Y. Li, X. Li and F. Xu, *NPG Asia Mater.*, 2019, **11**, 64.

150 S. T. Sanjay, W. Zhou, M. Dou, H. Tavakoli, L. Ma, F. Xu and X. Li, *Adv. Drug Delivery Rev.*, 2018, **128**, 3–28.

151 J. Zhang, X. Wei, R. Zeng, F. Xu and X. Li, *Future Sci. OA*, 2017, **3**, FSO187.

152 M. Lv, W. Zhou, H. Tavakoli, C. Bautista, J. Xia, Z. Wang and X. Li, *Biosens. Bioelectron.*, 2021, **176**, 112947.

153 W. Zhou, K. Hu, S. Kwee, L. Tang, Z. Wang, J. Xia and X. Li, *Anal. Chem.*, 2020, **92**, 2739–2747.

154 G. Fu, S. T. Sanjay, W. Zhou, R. A. Brekken, R. A. Kirken and X. Li, *Anal. Chem.*, 2018, **90**, 5930–5937.

155 G. Fu, S. T. Sanjay, M. Dou and X. Li, *Nanoscale*, 2016, **8**, 5422–5427.

156 K. S. Prasad, X. Cao, N. Gao, Q. Jin, S. T. Sanjay, G. Henao-Pabon and X. Li, *Sens. Actuators, B*, 2020, **305**, 127516.

157 S. K. Katla, J. Zhang, E. Castro, R. A. Bernal and X. Li, *ACS Appl. Mater. Interfaces*, 2018, **10**, 75–82.

158 X. Xu, X. Wang, J. Hu, Y. Gong, L. Wang, W. Zhou, X. Li and F. Xu, *Electrophoresis*, 2019, **40**, 914–921.

159 G. Fu, Y. Zhu, W. Wang, M. Zhou and X. Li, *ACS Sens.*, 2019, **4**, 2481–2490.